

Structure-Preserving Optimal Control of Open Quantum Systems via a Discrete Contact PMP

Leonardo J. Colombo*

Abstract

We develop a discrete Pontryagin Maximum Principle (PMP) for controlled open quantum systems governed by Lindblad dynamics, and introduce a second-order *contact Lie-group variational integrator* (contact LGVI) that preserves both the CPTP (completely positive and trace-preserving) structure of the Lindblad flow and the contact geometry underlying the discrete PMP. A type-II discrete contact generating function produces a strict discrete contactomorphism under which the state, costate, and cost propagate in exact agreement with the variational structure of the discrete contact PMP.

We apply this framework to the optimal control of a dissipative qubit and compare it with a non-geometric explicit RK2 discretization of the Lindblad equation. Although both schemes have the same formal order, the RK2 method accumulates geometric drift (loss of trace, positivity violations, and breakdown of the discrete contact form) that destabilizes PMP shooting iterations, especially under strong dissipation or long horizons. In contrast, the contact LGVI maintains exact CPTP structure and discrete contact geometry step by step, yielding stable, physically consistent, and geometrically faithful optimal control trajectories.

1 Introduction

The design of reliable numerical methods for simulation and optimal control of open quantum systems has become a central challenge in quantum information processing, quantum sensing, and dissipative quantum engineering [31, 1, 8, 9, 10, 13, 14]. At the level of density operators $\rho \in \mathbb{C}^{n \times n}$, the dynamics of an open quantum system with coherent control $u(t)$ are governed by a Lindblad master equation,

$$\dot{\rho}(t) = -i[H(u(t)), \rho(t)] + \sum_j L_j \rho(t) L_j^\dagger - \frac{1}{2}\{L_j^\dagger L_j, \rho(t)\},$$

the generator of a completely positive trace-preserving (CPTP) semigroup [22, 17, 11]. The physical state space,

$$\mathcal{D} = \{\rho \geq 0, \rho = \rho^\dagger, \text{tr}(\rho) = 1\},$$

is the convex ‘‘Bloch ball’’ in the qubit case; preserving positivity, trace, and Hermiticity at the discrete level is mandatory for obtaining physically meaningful simulations and control laws.

A second source of geometric structure enters when the system is optimized through an indirect method such as the Pontryagin Maximum Principle (PMP). The PMP introduces a costate P and an accumulated cost variable z , and the continuous-time extremals satisfy an extended system (ρ, P, z) evolving on a *contact manifold* [26, 15]. While the Lindblad equation itself is *not* a contact dynamical system, the PMP couples the forward dissipative dynamics of ρ with a backward evolution of observables P and a Herglotz-type evolution of the cost z , yielding a genuine contact Hamiltonian flow.

*Centre for Automation and Robotics, Spanish National Research Council (CSIC). Carretera de Campo Real, km 0, 200, 28500 Arganda del Rey, Spain. (leonardo.colombo@csic.es). The author acknowledges financial support from Grant PID2022-137909-NB-C22 funded by the Spanish Ministry of Science and Innovation.

This distinction is crucial. A numerical method for optimal control of open quantum systems must preserve *two* incompatible-looking structures: (i) the **quantum geometry** of the state evolution, requiring each discrete step to be CPTP; and (ii) the **optimal-control geometry** of the PMP, requiring the extended discrete map $(\rho_k, P_{k+1}, z_k) \mapsto (\rho_{k+1}, P_k, z_{k+1})$ to be a *discrete contactomorphism*.

If either structure is broken, the implications are severe: loss of positivity, trace drift, degradation of the stationarity conditions, ill-posed costate recursions, and ultimately failure of PMP shooting methods, especially on long horizons or under strong dissipation. These pathologies are consistent with classical results on geometric drift in non-structure-preserving schemes [18, 24, 21, 12].

Existing time-stepping methods for Lindblad dynamics include explicit and implicit Runge–Kutta schemes, commutator-free Magnus integrators, and Lie–group Runge–Kutta–Munthe–Kaas (RKMK) methods [19, 6, 25]. Although effective in short-time simulation, these integrators typically fail to preserve positivity or trace, thus violating CPTP structure; do not preserve the contact geometry of the PMP extended dynamics; accumulate large unphysical drift (negativity, trace explosion) under strong dissipation or long horizons; and produce costate instabilities that undermine the PMP stationarity conditions.

This motivates a fundamental question: *Can one construct a numerical method that simultaneously preserves (i) CPTP quantum dynamics and (ii) the contact geometry of the discrete PMP, thus providing a fully geometric integrator for optimal control of open quantum systems?* In this work we answer this question affirmatively.

In particular, the main contributions of this paper are the following:

(1) We derive a fully geometric **discrete contact PMP** on the quantum state space \mathcal{D} . We show that the discrete extremals arise from a type-II discrete contact Lagrangian and generating function, extending classical geometric PMP results [7, 4, 27, 5] to dissipative open quantum dynamics.

(2) We construct a second-order **contact Lie–group variational integrator** (contact LGVI) for Lindblad equations. The integrator combines exact Kraus maps for the dissipative subflow with exact Lie-group unitary propagators in a Strang splitting [29]. Each step is CPTP by construction and the extended PMP update is a discrete contactomorphism.

(3) We embed this LGVI into a discrete PMP shooting algorithm and compare it against a classical second-order non-contact integrator (RKMK). We demonstrate that preserving both CPTP and contact geometry is essential for numerical stability of the costate dynamics, the stationarity condition, and the maximization of the discrete Hamiltonian.

(4) Through numerical experiments, including long-horizon Lindblad simulation and optimal control of a dissipative qubit, we show that the contact LGVI avoids geometric drift, maintains physical constraints, and yields stable and accurate optimal control trajectories. By contrast, non-contact schemes exhibit severe positivity violations, trace explosion, and instability of the PMP iterations.

While variational and Lie-group methods for closed quantum systems are well-established, and geometric approaches to optimal control have been developed in symplectic and contact settings, a scheme that simultaneously preserves (i) CPTP Lindblad structure and (ii) the discrete contact geometry of the PMP appears to be absent from the literature. This paper unifies these two geometries and provides a robust framework for simulation and control of dissipative quantum systems.

2 Continuous-Time Contact Pontryagin Maximum Principle

In this section we recall the continuous-time Pontryagin Maximum Principle (PMP) in a form that makes explicit its contact-geometric structure. We also relate this formulation to the contact PMP of Ohsawa [26] and to the presymplectic/contact reduction of de León–Lainz–Muñoz–Lecanda

[15]. This provides the geometric foundation for the discrete-time construction presented in the next section.

2.1 Extended state space, contact form, and Hamiltonian

Let Q be a smooth manifold and U the set of admissible controls. We consider a control-affine system

$$\dot{x}(t) = f(x(t), u(t)), \quad x(t) \in Q, u(t) \in U, \quad (1)$$

and an optimal control problem of Bolza type with cost functional

$$J(u) := \int_0^T L(x(t), u(t)) dt + \Phi(x(T)), \quad (2)$$

where $L : Q \times U \rightarrow \mathbb{R}$ is the running cost and $\Phi : Q \rightarrow \mathbb{R}$ is a terminal (Mayer) cost.

Introduce the *cost accumulator* $z(t)$ defined by

$$\dot{z}(t) = L(x(t), u(t)), \quad z(0) = 0, \quad (3)$$

so that $z(T) = \int_0^T L(x(t), u(t)) dt$.

The natural geometric space for the PMP is the extended manifold $M := T^*Q \times \mathbb{R}$, with coordinates (x, p, z) , where $p \in T_x^*Q$ is the costate. We endow M with the canonical contact 1-form

$$\theta := dz - \langle p, dx \rangle.$$

Introduce the *cost accumulator* $z(t)$ via

$$\dot{z}(t) = L(x(t), u(t)), \quad z(0) = 0,$$

so that $z(T) = \int_0^T L(x(t), u(t)) dt$.

The *control Hamiltonian* is the map

$$H : (T^*Q \times \mathbb{R}) \times U \rightarrow \mathbb{R}, \quad H(x, p, z, u) := \langle p, f(x, u) \rangle + L(x, u),$$

which in particular is independent of z . This convention corresponds to the usual finite-dimensional Lagrange multiplier derivation and is equivalent to the more classical choice $H_c(x, p, z, u) = \langle p, f(x, u) \rangle - L(x, u)$ up to a change of sign of the cost multiplier.

The *maximized Hamiltonian* is

$$\mathcal{H}(x, p, z) := \sup_{u \in U} H(x, p, z, u),$$

assumed to be attained for the optimal control $u^*(t)$.

The PMP states that, if u^* is optimal, then there exists a nontrivial costate trajectory $p(t) \in T_{x(t)}^*Q$ such that $(x^*(t), p(t), z^*(t))$ satisfies the following system on the contact manifold (M, θ) :

$$\dot{x}(t) = \partial_p H_c(x(t), p(t), z(t), u^*(t)), \quad (4a)$$

$$\dot{p}(t) = -\partial_x H_c(x(t), p(t), z(t), u^*(t)), \quad (4b)$$

$$\dot{z}(t) = \langle p(t), \partial_p H_c(x(t), p(t), z(t), u^*(t)) \rangle - H_c(x(t), p(t), z(t), u^*(t)). \quad (4c)$$

The control is characterized almost everywhere by the *pointwise maximum condition*

$$u^*(t) \in \arg \max_{v \in U} H_c(x(t), p(t), z(t), v). \quad (5)$$

For a Bolza-type terminal cost $\Phi(x(T))$ and fixed final time T , the *transversality condition* is the standard one:

$$p(T) = d_x \Phi(x(T)), \quad z(T) \text{ free.} \quad (6)$$

No additional boundary conditions arise for $z(T)$, since the total cost is precisely the value of $z(T)$.

Using that $\partial_p H_c(x, p, z, u) = f(x, u)$ and that $H_c(x, p, z, u) = \langle p, f(x, u) \rangle - L(x, u)$, equation (4c) reduces to

$$\dot{z}(t) = L(x(t), u^*(t)),$$

as expected.

Next, let X_{H_c} be the vector field on M defined by (4a)–(4c). A direct computation using Cartan's identity $\mathcal{L}_X \theta = \iota_X(d\theta) + d(\iota_X \theta)$ shows that

$$\mathcal{L}_{X_{H_c}} \theta = (\partial_z H_c) \theta. \quad (7)$$

Equation (7) is the defining property of a (cooriented) *contact Hamiltonian vector field* on (M, θ) : for a contact Hamiltonian H , the identities

$$\iota_{X_H} \theta = -H, \quad \iota_{X_H} d\theta = dH - (\partial_z H) \theta$$

imply precisely $\mathcal{L}_{X_H} \theta = (\partial_z H) \theta$. Since in our setting H_c is independent of z , we have $\partial_z H_c = 0$ and therefore

$$\mathcal{L}_{X_{H_c}} \theta = 0,$$

so the PMP flow preserves the contact structure on (M, θ) . Therefore, the PMP flow is a *contact Hamiltonian trajectory* on (M, θ) in the sense of standard contact geometry [16].

This explicit contact viewpoint is equivalent, in the normal case, to the contact-geometric PMP of Ohsawa [26], where the contact structure is written on the projectivized cotangent bundle $P(T^*(\mathbb{R} \times Q))$, and to the reduced contact structure of the presymplectic framework developed in [15]. Working directly on $(T^*Q \times \mathbb{R}, \theta)$ provides a simpler coordinate model that is particularly suitable for deriving a discrete contact PMP.

Remark 1 (Relation to Ohsawa's contact PMP). Ohsawa [26] formulates the continuous-time PMP as a contact Hamiltonian system on the projectivized cotangent bundle $P(T^*(\mathbb{R} \times Q))$, where the running cost x_0 is treated as an extended state and the costate is represented projectively. In local coordinates (x_0, x, λ) , the canonical contact form $-dx_0 + \lambda dx$ and the associated contact Hamiltonian reproduce exactly the classical PMP equations.

Identifying $z = x_0$, $p = \lambda$ and $\theta = dz - p dx$, our formulation on $M = T^*Q \times \mathbb{R}$ corresponds to the normal chart of Ohsawa's contact manifold (i.e. where the projective costate has $\nu_0 \neq 0$). We adopt this “deprojectivized” representation because it provides a simpler local model that is particularly convenient for the discrete contact construction introduced in the next section. \diamond

Remark 2 (Relation to the presymplectic/contact approach of de León–Lainz–Muñoz-Lecanda). De León, Lainz and Muñoz-Lecanda [15] formulate the PMP as a presymplectic Hamiltonian system on $T^*(\mathbb{R} \times Q)$ and show that, for normal extremals, the dynamics reduce to a contact Hamiltonian system on an appropriate submanifold. Abnormal extremals remain presymplectic and do not share the same contact structure.

Our formulation works directly with the contact manifold $M = T^*Q \times \mathbb{R}$ and the form $\theta = dz - p dx$, which corresponds (in the normal case) to the reduced contact structure of [15]. This simplified local model is the one we discretize in the next section. \diamond

The discrete-time Pontryagin Maximum Principle was developed primarily by Boltyanskii (see [7] and the references therein) and discrete time is the setting of our current work. Discrete formulations of the PMP on manifolds, such as the formers and the geometric approach of

Assif–Chatterjee–Banavar [4], provide discrete adjoint and stationarity conditions but do not enforce preservation of the underlying contact structure of the continuous PMP. Consequently, naïve discretizations may distort the geometry, especially over long horizons. In the next section we develop a discrete PMP whose update map is a *discrete contactomorphism*, yielding a structure-preserving analogue of the continuous contact PMP and a natural discrete counterpart to Ohsawa’s contact formulation.

3 A Discrete Contact PMP on Manifolds

We now construct a discrete counterpart of the continuous-time contact PMP developed in Section 2. Our formulation improves upon the geometric discrete PMP of Assif–Chatterjee–Banavar [4] by making the underlying contact geometry explicit. Following the philosophy of discrete contact variational principles [30, 2], the discrete state–costate update is obtained from a discrete *contact generating function*. As a consequence, the resulting discrete PMP map is a genuine *discrete contactomorphism*, thus retaining the geometric structure of the continuous contact Hamiltonian flow rather than providing merely first-order optimality conditions.

Let $t_k = k\Delta t$, $k = 0, \dots, N$, and $T = N\Delta t$. The control is a sequence $\{u_k\}_{k=0}^{N-1}$ with $u_k \in U$, and the state evolves on a smooth manifold Q .

We assume discrete dynamics of the form

$$x_{k+1} = F(x_k, u_k), \quad (8)$$

where $F : Q \times U \rightarrow Q$ is a C^1 map and x_0 is fixed.

The discrete Bolza cost functional is

$$J_d(\{u_k\}) = \sum_{k=0}^{N-1} L_d(x_k, u_k) + \Phi(x_N). \quad (9)$$

In contrast to standard discretizations where $L_d(x, u) = L(x, u)\Delta t + O(\Delta t^2)$ is chosen ad hoc, we take L_d to be a consistent approximation of the *exact discrete contact Lagrangian* associated with the continuous contact PMP flow, in the sense of [30, 2]. This ensures that the resulting discrete scheme preserves the contact geometry.

As in the continuous case, we introduce an accumulated cost variable:

$$z_{k+1} = z_k + L_d(x_k, u_k), \quad z_0 = 0. \quad (10)$$

Since L_d approximates $\int_{t_k}^{t_{k+1}} L(x(t), u(t)) dt$, the time step Δt is already incorporated, and no explicit factor appears in (10). The extended discrete state is $(x_k, z_k) \in Q \times \mathbb{R}$.

Let $p_{k+1} \in T_{x_{k+1}}^* Q$ denote the discrete costate associated with the constraint $x_{k+1} = F(x_k, u_k)$. We introduce the *discrete contact Hamiltonian*

$$H_d(x_k, p_{k+1}, z_k, u_k) := \langle p_{k+1}, F(x_k, u_k) \rangle + L_d(x_k, u_k), \quad (11)$$

which is a smooth map

$$H_d : T^* Q \times \mathbb{R} \times U \rightarrow \mathbb{R}, \quad (x_k, p_{k+1}, z_k, u_k) \mapsto H_d(x_k, p_{k+1}, z_k, u_k).$$

We also define the associated type-II *discrete contact generating function*

$$S_d(x_k, p_{k+1}, z_k, u_k) := z_k + L_d(x_k, u_k) + \langle p_{k+1}, F(x_k, u_k) - x_k \rangle. \quad (12)$$

Note that H_d does not depend on the cost variable z_k , so we may occasionally write $H_d(x_k, p_{k+1}, u_k)$ for brevity. Its domain is still $T^* Q \times \mathbb{R} \times U$, but the dependence on z_k is trivial.

Furthermore, differentiation with respect to the control variable yields

$$\partial_u S_d(x_k, p_{k+1}, z_k, u_k) = \partial_u L_d(x_k, u_k) + \langle p_{k+1}, \partial_u F(x_k, u_k) \rangle = \partial_u H_d(x_k, p_{k+1}, z_k, u_k). \quad (13)$$

Hence the stationarity conditions $\partial_u S_d = 0$ and $\partial_u H_d = 0$ are equivalent.

The specific combination of terms in S_d is not arbitrary. In the continuous contact PMP, the identity $\dot{z} = \langle p, \dot{x} \rangle - H_c(x, p, z, u)$ characterizes contact Hamiltonian flows. Up to the sign convention on the cost multiplier, this can be rewritten using a Hamiltonian of the form $\tilde{H}(x, p, u) = \langle p, f(x, u) \rangle + L(x, u)$, which is the natural form arising from the finite-dimensional Lagrange multiplier derivation. Our discrete Hamiltonian H_d follows this latter convention.

The discrete generating function S_d reproduces the same structural pattern: it contains z_k , the discrete analogue of the accumulated cost, and the term $\langle p_{k+1}, F(x_k, u_k) - x_k \rangle + L_d(x_k, u_k)$ in exactly the same additive configuration as in the continuous identity. Moreover, a direct computation using (11) and (12) gives

$$\partial_x S_d(x_k, p_{k+1}, z_k, u_k) = \partial_x H_d(x_k, p_{k+1}, z_k, u_k) - p_{k+1}, \quad (14)$$

so that the adjoint recursion can be written equivalently as

$$p_k - p_{k+1} = \partial_x S_d(x_k, p_{k+1}, z_k, u_k).$$

Next, we define the extended discrete manifold $M_d := T^*Q \times \mathbb{R}$ and, for each time index k , the discrete contact form

$$\Theta_k := dz_k - \langle p_k, dx_k \rangle, \quad (15)$$

which is the exact discrete analogue of the continuous contact form $\theta = dz - \langle p, dx \rangle$. Differentiating (12) and using (15) yields the discrete contact identity

$$dS_d = \Theta_k + \langle p_{k+1}, dx_{k+1} \rangle - \Theta_{k+1}, \quad (16)$$

an identity valid on the extended space with coordinates $(x_k, p_k, z_k, x_{k+1}, p_{k+1}, z_{k+1})$ before imposing the discrete dynamics. This is the discrete analogue of the continuous contact identity $\mathcal{L}_{X_H} \theta = (\partial_z H) \theta$ and will be used below to prove that the resulting PMP update map is a discrete contactomorphism.

We now state the discrete analogue of the contact PMP.

Theorem 1. *Let $\{u_k^*\}_{k=0}^{N-1}$ be optimal for the discrete problem. Then there exists a non-trivial costate sequence $\{p_k^*\}_{k=1}^N$, $p_k^* \in T_{x_k^*}^* Q$, such that for $k = 0, \dots, N-1$, the quadruple $(x_k^*, p_{k+1}^*, z_k^*, u_k^*)$ satisfies:*

1. *State and cost updates:*

$$x_{k+1}^* = F(x_k^*, u_k^*), \quad (17a)$$

$$z_{k+1}^* = z_k^* + L_d(x_k^*, u_k^*). \quad (17b)$$

2. *Adjoint equation:* for $k = 1, \dots, N-1$,

$$p_k^* = \partial_x L_d(x_k^*, u_k^*) + (\partial_x F(x_k^*, u_k^*))^* p_{k+1}^*, \quad (18)$$

or equivalently

$$p_k^* = \partial_x H_d(x_k^*, p_{k+1}^*, z_k^*, u_k^*), \quad (19)$$

and, using (14),

$$p_k^* - p_{k+1}^* = \partial_x S_d(x_k^*, p_{k+1}^*, z_k^*, u_k^*). \quad (20)$$

3. *Terminal condition:*

$$p_N^* = d_x \Phi(x_N^*). \quad (21)$$

4. *Stationarity:*

$$\partial_u H_d(x_k^*, p_{k+1}^*, z_k^*, u_k^*) = 0, \quad k = 0, \dots, N-1, \quad (22)$$

or, under the standing continuity and compactness assumptions,

$$u_k^* \in \arg \max_{u \in U} H_d(x_k^*, p_{k+1}^*, z_k^*, u), \quad (23)$$

for $k = 0, \dots, N-1$.

Proof. We use the classical finite-dimensional Lagrange multiplier theorem in local coordinates on Q (see, e.g., [28]); see also [4] for a related argument in a purely geometric setting.

Fix $x_0 \in Q$, a time step $\Delta t > 0$ and an integer $N \in \mathbb{N}$ defining the horizon $T = N\Delta t$. An admissible discrete trajectory is completely determined by the sequence of states x_1, \dots, x_N and controls u_0, \dots, u_{N-1} satisfying the discrete dynamics

$$x_{k+1} = F(x_k, u_k), \quad k = 0, \dots, N-1. \quad (24)$$

The discrete cost is

$$J_d(\{x_k, u_k\}) = \sum_{k=0}^{N-1} L_d(x_k, u_k) + \Phi(x_N),$$

and the accumulated cost variable z_k is defined by

$$z_{k+1} = z_k + L_d(x_k, u_k), \quad z_0 = 0,$$

so it does not introduce additional constraints.

We assume throughout that U is a compact subset of a finite-dimensional vector space, that F and L_d are C^1 , and that Φ is C^1 . Under these assumptions, the discrete optimal control problem reduces to a finite-dimensional constrained optimization problem with decision variables $(x_1, \dots, x_N, u_0, \dots, u_{N-1})$, equality constraints given by (24), and cost functional J_d as above.

We focus on a *normal* optimal solution, i.e. one to which the usual Lagrange multiplier theorem applies with nonzero cost multiplier; this excludes pathological abnormal extremals and is standard in PMP theory.

Let $\{x_k^*\}_{k=0}^N$ and $\{u_k^*\}_{k=0}^{N-1}$ be an optimal trajectory and control sequence. Since Q is a smooth manifold and the time horizon is finite, we may choose coordinate charts $\varphi_k : U_k \rightarrow \mathbb{R}^n$ with $x_k^* \in U_k$ for $k = 0, \dots, N$, such that the image of x_k^* lies in the interior of $\varphi_k(U_k)$. Working in these local coordinates, we identify $\xi_k := \varphi_k(x_k) \in \mathbb{R}^n$, and rewrite $F(x_k, u_k)$ as a smooth map $\widehat{F}_k(\xi_k, u_k)$ taking values in \mathbb{R}^n . Similarly, L_d and Φ are expressed in local coordinates as smooth maps on $\mathbb{R}^n \times U$ and \mathbb{R}^n , respectively. Since the Lagrange multiplier conditions are coordinate-invariant, it suffices to derive them in this local representation.

In these coordinates, the discrete optimization problem becomes

$$\min \widehat{J}_d(\{\xi_k, u_k\}) := \sum_{k=0}^{N-1} \widehat{L}_d(\xi_k, u_k) + \widehat{\Phi}(\xi_N),$$

subject to

$$\xi_{k+1} = \widehat{F}_k(\xi_k, u_k), \quad k = 0, \dots, N-1, \quad (25)$$

with ξ_0 fixed.

We now apply the classical finite-dimensional Lagrange multiplier theorem for equality constraints. Define the constraint map

$$G_k(\xi_k, u_k, \xi_{k+1}) := \widehat{F}_k(\xi_k, u_k) - \xi_{k+1} \in \mathbb{R}^n, \quad k = 0, \dots, N-1.$$

The full constraint map is

$$G(\{\xi_k, u_k\}) := (G_0, \dots, G_{N-1}) \in (\mathbb{R}^n)^N.$$

Since G is C^1 and the feasible set is nonempty, the usual Lagrange multiplier theorem guarantees the existence of multipliers $\{\lambda_{k+1}\}_{k=0}^{N-1} \subset (\mathbb{R}^n)^*$ and a scalar $\alpha \in \mathbb{R}$ (cost multiplier) such that, at the optimum,

$$\alpha D\widehat{J}_d + \sum_{k=0}^{N-1} \lambda_{k+1}^\top D G_k = 0.$$

Normality means $\alpha \neq 0$, and we normalize by setting $\alpha = 1$. The multipliers λ_{k+1} will give, after identification via the charts, the covectors $p_{k+1}^* \in T_{x_{k+1}^*}^* Q$.

Equivalently, introducing the augmented functional

$$\widehat{\mathbb{J}}_d = \sum_{k=0}^{N-1} \left(\widehat{L}_d(\xi_k, u_k) + \lambda_{k+1}^\top (\widehat{F}_k(\xi_k, u_k) - \xi_{k+1}) \right) + \widehat{\Phi}(\xi_N),$$

first-order optimality reads $\partial_{\xi_k} \widehat{\mathbb{J}}_d = 0$ for $k = 1, \dots, N$, and $\partial_{u_k} \widehat{\mathbb{J}}_d = 0$ for $k = 0, \dots, N-1$.

For each k , differentiation of $\widehat{\mathbb{J}}_d$ with respect to λ_{k+1} yields

$$0 = \partial_{\lambda_{k+1}} \widehat{\mathbb{J}}_d = \widehat{F}_k(\xi_k, u_k) - \xi_{k+1},$$

i.e. the constraint (25). Translating back to Q , this is precisely $x_{k+1} = F(x_k, u_k)$, which proves the state equation in the theorem. The cost update $z_{k+1} = z_k + L_d(x_k, u_k)$ holds by definition of z_k .

For $k = 1, \dots, N-1$, the derivative of $\widehat{\mathbb{J}}_d$ with respect to ξ_k gives

$$0 = \partial_{\xi_k} \widehat{\mathbb{J}}_d = \partial_{\xi_k} \widehat{L}_d(\xi_k, u_k) + (\partial_{\xi_k} \widehat{F}_k(\xi_k, u_k))^\top \lambda_{k+1} - \lambda_k.$$

Rearranging,

$$\lambda_k = \partial_{\xi_k} \widehat{L}_d(\xi_k, u_k) + (\partial_{\xi_k} \widehat{F}_k(\xi_k, u_k))^\top \lambda_{k+1}.$$

Pulling this back via the charts yields, in intrinsic notation,

$$p_k = \partial_x L_d(x_k, u_k) + (\partial_x F(x_k, u_k))^* p_{k+1},$$

where $p_k \in T_{x_k}^* Q$ is the covector corresponding to λ_k . This is exactly the adjoint recursion (18).

Using the definition (11) of H_d , one computes

$$\partial_x H_d(x_k, p_{k+1}, z_k, u_k) = \partial_x \langle p_{k+1}, F(x_k, u_k) \rangle + \partial_x L_d(x_k, u_k) = (\partial_x F(x_k, u_k))^* p_{k+1} + \partial_x L_d(x_k, u_k),$$

so the previous relation is equivalently written as

$$p_k = \partial_x H_d(x_k, p_{k+1}, z_k, u_k),$$

and, by (14), as

$$p_k - p_{k+1} = \partial_x S_d(x_k, p_{k+1}, z_k, u_k),$$

which gives (20).

Similarly, differentiation of $\widehat{\mathbb{J}}_d$ with respect to ξ_N yields

$$0 = \partial_{\xi_N} \widehat{\mathbb{J}}_d = \partial_{\xi_N} \widehat{\Phi}(\xi_N) - \lambda_N,$$

so $\lambda_N = \partial_{\xi_N} \widehat{\Phi}(\xi_N)$, i.e. $p_N = d_x \Phi(x_N)$, which gives the terminal condition in the theorem.

For each $k = 0, \dots, N-1$, the derivative with respect to u_k is

$$0 = \partial_{u_k} \widehat{\mathbb{J}}_d = \partial_{u_k} \widehat{L}_d(\xi_k, u_k) + (\partial_{u_k} \widehat{F}_k(\xi_k, u_k))^{\top} \lambda_{k+1}.$$

In intrinsic notation this reads

$$0 = \partial_u L_d(x_k, u_k) + (\partial_u F(x_k, u_k))^* p_{k+1}.$$

Using the definition (11) of H_d ,

$$\partial_u H_d(x_k, p_{k+1}, z_k, u_k) = (\partial_u F(x_k, u_k))^* p_{k+1} + \partial_u L_d(x_k, u_k),$$

so the first-order condition above is equivalent to

$$\partial_u H_d(x_k, p_{k+1}, z_k, u_k) = 0,$$

which is (22). Under the standing assumptions (continuity of H_d in u , compactness of U) this first-order condition is equivalent to

$$u_k \in \arg \max_{u \in U} H_d(x_k, p_{k+1}, z_k, u),$$

which is the maximum condition (23).

The Lagrange multiplier theorem implies that the pair consisting of the cost multiplier α and the constraint multipliers $\{\lambda_k\}$ cannot be trivial. Under the normality assumption, we have $\alpha \neq 0$, which we normalized to $\alpha = 1$. Therefore the sequence $\{\lambda_k\}$, and hence $\{p_k\}$, cannot vanish identically. This yields a nontrivial costate sequence $\{p_k^*\}_{k=1}^N$ associated with the optimal control $\{u_k^*\}_{k=0}^{N-1}$.

Collecting all the conditions above and reverting to the original notation, we obtain exactly the system stated in Theorem 1. \square

Remark 3. If the Lagrange multiplier associated with the cost functional vanishes, i.e. $\alpha = 0$ in the finite-dimensional multiplier theorem, the discrete PMP reduces to the system obtained by removing all terms involving L_d and Φ . The adjoint recursion becomes

$$p_k = (\partial_x F(x_k, u_k))^* p_{k+1},$$

and the stationarity condition reduces to

$$(\partial_u F(x_k, u_k))^* p_{k+1} = 0.$$

Such extremals do not see the cost and depend only on the geometry of the constraint $x_{k+1} = F(x_k, u_k)$. In many practical situations they are excluded automatically because, for each k , the map $u \mapsto F(x_k, u)$ has full rank in the control directions, forcing $p_{k+1} = 0$ and hence triviality of the entire multiplier sequence. \diamond

Remark 4. The regularity assumption $F \in C^1(Q \times U, Q)$ is the minimal smoothness required for the discrete PMP. Indeed, the discrete Hamiltonian H_d and the contact generating function S_d involve derivatives with respect to x_k and u_k , and the adjoint update (18) contains the term $\partial_x F(x_k, u_k)$. Thus differentiability of F is necessary and sufficient for the variational derivation of the discrete PMP, for the definition of the discrete costate recursion, and for the validity of the stationarity condition. Higher regularity (e.g. C^2) is only required for error analysis, not for the first-order optimality theory or the discrete contactomorphism property. \diamond

The discrete PMP update map is $\Psi_k : (x_k, p_{k+1}, z_k) \rightarrow (x_{k+1}, p_k, z_{k+1})$, where the triple (x_{k+1}, p_k, z_{k+1}) is defined implicitly by

$$x_{k+1} = F(x_k, u_k), \quad (26a)$$

$$z_{k+1} = z_k + L_d(x_k, u_k), \quad (26b)$$

$$p_k - p_{k+1} = \partial_{x_k} S_d(x_k, p_{k+1}, z_k, u_k), \quad (26c)$$

$$0 = \partial_{u_k} S_d(x_k, p_{k+1}, z_k, u_k), \quad (26d)$$

and $u_k \in U$ is determined by the stationarity condition $\partial_{u_k} S_d(x_k, p_{k+1}, z_k, u_k) = 0$. Using $\partial_u S_d = \partial_u H_d$ from (13), this is equivalent to the discrete condition $\partial_u H_d = 0$ and, under the standing compactness assumptions, to the maximization condition (23).

Note that (26a) and (26c) are consistent with the discrete PMP equations in Theorem 1, since

$$\partial_{p_{k+1}} S_d(x_k, p_{k+1}, z_k, u_k) = F(x_k, u_k) - x_k,$$

so that (26a) can be rewritten as

$$x_{k+1} - x_k = \partial_{p_{k+1}} S_d(x_k, p_{k+1}, z_k, u_k),$$

and (26c) is precisely the equivalent form (20) of the adjoint recursion.

Only the control u_k is obtained from a maximization of S_d (or H_d), while x_{k+1} , p_k , and z_{k+1} follow from the discrete dynamics and the adjoint/contact equations generated by S_d .

Remark 5. The discrete adjoint equation involves p_{k+1} rather than p_k because the discrete constraint $x_{k+1} = F(x_k, u_k)$ introduces its Lagrange multiplier at the future node. This mirrors the continuous PMP, in which $p(t)$ satisfies a terminal boundary condition and evolves backward in time. In the language of discrete contact and Hamilton–Jacobi theory, the function $S_d(x_k, p_{k+1}, z_k, u_k)$ plays the role of a type-II generating function, which naturally defines the update map $(x_k, p_{k+1}) \mapsto (x_{k+1}, p_k)$ after eliminating u_k and z_k . \diamond

Theorem 2. *For each k , the discrete PMP map Ψ_k satisfies*

$$\Psi_k^* \Theta_{k+1} = \Theta_k. \quad (27)$$

Thus Ψ_k is a strict discrete contactomorphism, preserving the discrete family of contact forms $\{\Theta_k\}$ on M_d .

Proof. Differentiating (12) and using the definition of Θ_k in (15) yields the discrete contact identity (16),

$$dS_d = \Theta_k + \langle p_{k+1}, dx_{k+1} \rangle - \Theta_{k+1},$$

an identity valid on the extended space with coordinates $(x_k, p_k, z_k, x_{k+1}, p_{k+1}, z_{k+1})$ before imposing the discrete dynamics.

On the graph of the update map Ψ_k , the variables (x_{k+1}, p_k, z_{k+1}) are expressed in terms of (x_k, p_{k+1}, z_k) by (26), and the control u_k is determined by the stationarity condition (26d). Restricting (16) to this graph and using (26a)–(26b) to eliminate dx_{k+1} and dz_{k+1} yields

$$dS_d = \Theta_k - \Psi_k^* \Theta_{k+1},$$

where now S_d is viewed as a function of the independent variables (x_k, p_{k+1}, z_k) .

By construction, S_d is a type-II contact generating function for the map Ψ_k ; the stationarity condition (26d) eliminates the dependence on the control, so dS_d is an exact 1-form on the parameter space of the graph. Hence the identity above implies $\Psi_k^* \Theta_{k+1} = \Theta_k$, which is (27).

Since H_d (and therefore S_d) is independent of the cost variable z_k , the associated discrete contact vector field has vanishing $\partial_z H_d$. Consequently, the contactomorphism Ψ_k preserves the discrete contact form exactly, with no conformal factor. This is the discrete analogue of the strict contact case for the continuous PMP discussed in Section 2. \square

Remark 6. Assif–Chatterjee–Banavar [4] obtained a discrete PMP on manifolds, but without identifying or enforcing preservation of the contact structure. Theorem 2 shows that our discrete PMP map preserves the discrete contact form exactly, matching the continuous property $\mathcal{L}_{X_H}\theta = (\partial_z H)\theta$ and providing a structure-preserving discretization of the contact PMP. \diamond

Remark 7. The discrete contact structure is intrinsically tied to the *normal* case. When the cost multiplier $\alpha \neq 0$, the discrete PMP is generated by the type-II contact generating function S_d , and the update map Ψ_k is a strict discrete contactomorphism (Theorem 2).

In contrast, for abnormal extremals ($\alpha = 0$) the cost functional plays no role and all terms involving L_d and Φ disappear. The resulting dynamics satisfy only

$$p_k = (\partial_x F(x_k, u_k))^* p_{k+1}, \quad (\partial_u F(x_k, u_k))^* p_{k+1} = 0,$$

which define a *presymplectic* rather than contact update map. This mirrors precisely the continuous-time situation studied by de León–Lainz–Muñoz–Lecanda, where abnormal extremals live on a presymplectic PMP manifold and cannot be captured by a contact reduction. Thus the discrete theory reproduces the same geometric dichotomy: normal extremals are contact, abnormal ones presymplectic. \diamond

4 Contact Lie–Group Variational Integrators

In this section we adapt the contact–geometric framework of Section 3 to the case where the configuration manifold is a Lie group G . We work in left–trivialized coordinates and construct retraction–based Lie–group contact variational integrators. These integrators will later be combined with the discrete contact PMP to obtain structure–preserving schemes for optimal control on G , and in particular on $SU(2)$. Throughout this section, all trivializations of TG and T^*G are understood to be left–trivializations unless explicitly stated otherwise.

Throughout, \mathfrak{g} denotes the Lie algebra of G . We denote by

$$L_g : G \rightarrow G, \quad L_g(h) = gh, \quad R_g : G \rightarrow G, \quad R_g(h) = hg,$$

the left and right translations by $g \in G$. Their tangent maps at the identity are

$$T_e L_g : \mathfrak{g} \rightarrow T_g G, \quad T_e R_g : \mathfrak{g} \rightarrow T_g G,$$

and the corresponding dual maps (used to left– and right–trivialize cotangent vectors) are

$$T_e^* L_g : T_g^* G \rightarrow \mathfrak{g}^*, \quad T_e^* R_g : T_g^* G \rightarrow \mathfrak{g}^*.$$

The adjoint representation of G on its Lie algebra \mathfrak{g} is defined by

$$\text{Ad}_g := T_e(L_g \circ R_{g^{-1}}) : \mathfrak{g} \rightarrow \mathfrak{g},$$

and its dual action by $\text{Ad}_g^* : \mathfrak{g}^* \rightarrow \mathfrak{g}^*$.

4.1 Contact Lagrangian systems on Lie groups

Let G be a Lie group with Lie algebra \mathfrak{g} , and let $L : TG \times \mathbb{R} \rightarrow \mathbb{R}$ be a (regular) contact Lagrangian in the sense of [3]. Using the standard left trivialization

$$TG \times \mathbb{R} \simeq G \times \mathfrak{g} \times \mathbb{R}, \quad (g, \dot{g}, z) \mapsto (g, \xi, z), \quad \xi := T_g L_{g^{-1}}(\dot{g}),$$

we obtain the *left–trivialized contact Lagrangian*

$$\tilde{L} : G \times \mathfrak{g} \times \mathbb{R} \rightarrow \mathbb{R}, \quad \tilde{L}(g, \xi, z) := L(g, \dot{g}, z), \quad \dot{g} = T_e L_g(\xi).$$

For simplicity of notation, we will write $L(g, \xi, z)$ instead of \tilde{L} from now on.

The dynamics of the contact Lagrangian system on $TG \times \mathbb{R}$ can be expressed, in these left-trivialized coordinates, by the following *Euler–Poincaré–Herglotz* equations on $G \times \mathfrak{g} \times \mathbb{R}$ (cf. Theorem 4.1 in [3]):

$$\dot{g} = T_e \mathbf{L}_g(\xi), \quad (28a)$$

$$\dot{z} = L(g, \xi, z), \quad (28b)$$

$$\frac{d}{dt} \left(\frac{\delta L}{\delta \xi}(g, \xi, z) \right) = \text{ad}_\xi^* \left(\frac{\delta L}{\delta \xi}(g, \xi, z) \right) + T_e^* \mathbf{L}_g \left(\frac{\delta L}{\delta g}(g, \xi, z) \right) + \frac{\delta L}{\delta \xi}(g, \xi, z) \frac{\partial L}{\partial z}(g, \xi, z). \quad (28c)$$

Here $\delta L / \delta \xi \in \mathfrak{g}^*$ is the functional derivative with respect to the Lie-algebra variable, $\delta L / \delta g \in T_g^*G$ is the derivative with respect to g , $\text{ad}_\xi^* : \mathfrak{g}^* \rightarrow \mathfrak{g}^*$ is the coadjoint action, and $T_e^* \mathbf{L}_g : T_g^*G \rightarrow \mathfrak{g}^*$ is as above.

Defining the *body momentum* $\mu := \frac{\delta L}{\delta \xi}(g, \xi, z) \in \mathfrak{g}^*$, equation (28c) can be written more compactly as

$$\dot{\mu} = \text{ad}_\xi^* \mu + T_e^* \mathbf{L}_g \left(\frac{\delta L}{\delta g} \right) + \mu \frac{\partial L}{\partial z}, \quad \xi = T_g \mathbf{L}_{g^{-1}}(\dot{g}), \quad \dot{z} = L(g, \xi, z). \quad (29)$$

Assuming L is *hyperregular* (so that the fiber derivative $\mathbb{F}L : TG \times \mathbb{R} \rightarrow T^*G \times \mathbb{R}$ is a global diffeomorphism), one defines the left-trivial Legendre transform

$$\mathbb{F}L : G \times \mathfrak{g} \times \mathbb{R} \rightarrow G \times \mathfrak{g}^* \times \mathbb{R}, \quad \mathbb{F}L(g, \xi, z) = (g, \mu, z), \quad \mu = \frac{\delta L}{\delta \xi}(g, \xi, z),$$

and the associated *contact Hamiltonian*

$$H : G \times \mathfrak{g}^* \times \mathbb{R} \rightarrow \mathbb{R}, \quad H(g, \mu, z) := \langle \mu, \xi \rangle - L(g, \xi, z), \quad \mu = \frac{\delta L}{\delta \xi}(g, \xi, z).$$

The Legendre transform is a contactomorphism between $(TG \times \mathbb{R}, \eta_L)$ and $(T^*G \times \mathbb{R}, \theta)$, where

$$\eta_L = dz - \theta_L, \quad \theta_L = (\mathbb{F}L)^*(\theta_G), \quad \theta_G = \langle p, g^{-1}dg \rangle$$

is the left-trivialized canonical 1-form on T^*G , and

$$\theta = dz - \theta_G$$

is the canonical contact form on $T^*G \times \mathbb{R}$. In particular, the vector field ξ_L solving the Euler–Poincaré–Herglotz equations (28) is $\mathbb{F}L$ -related to the contact Hamiltonian vector field X_H on $(T^*G \times \mathbb{R}, \theta)$:

$$(\mathbb{F}L)_*(\xi_L) = X_H \circ \mathbb{F}L,$$

and the resulting flow satisfies the identity

$$\mathcal{L}_{X_H} \theta = (\partial_z H) \theta.$$

Remark 8. In the special case of a left-invariant contact Lagrangian, $L(g, \xi, z) = \ell(\xi, z)$, the term $T_e^* \mathbf{L}_g(\delta L / \delta g)$ vanishes and (29) reduces to the *Euler–Poincaré–Herglotz* equations on $\mathfrak{g} \times \mathbb{R}$:

$$\dot{\mu} = \text{ad}_\xi^* \mu + \mu \frac{\partial \ell}{\partial z}(\xi, z), \quad \dot{z} = \ell(\xi, z), \quad \mu = \frac{\partial \ell}{\partial \xi}(\xi, z).$$

This is precisely the reduced form obtained in [3], and it will be the relevant setting for our Lie-group variational integrators. \diamond

4.2 Exact discrete contact Lagrangian and order of a contact LGVI

Let $h > 0$ be a fixed time step. Let $L : G \times \mathfrak{g} \times \mathbb{R} \rightarrow \mathbb{R}$ be a smooth left-trivialized contact Lagrangian, and let $(g(t), \xi(t), z(t))$ with $t \in [0, h]$ be the unique solution of the Euler–Poincaré–Herglotz equations (28) with boundary conditions $g(0) = g_k$, $z(0) = z_k$ and $g(h) = g_{k+1}$ for $h > 0$ small enough. Existence and uniqueness hold under the usual regularity and hyperregularity assumptions on L .

The *exact discrete contact Lagrangian* is then defined by

$$L_h^e(g_k, g_{k+1}, z_k) := \int_0^h L(g(t), \xi(t), z(t)) dt, \quad (30)$$

where $(g(t), \xi(t), z(t))$ is as above.

Proposition 1. *Let L_h^e be given by (30). Define the discrete action sum*

$$\mathcal{S}_d = \sum_{k=0}^{N-1} L_h^e(g_k, g_{k+1}, z_k),$$

with z_k determined recursively by

$$z_{k+1} = z_k + L_h^e(g_k, g_{k+1}, z_k), \quad z_0 \text{ given.} \quad (31)$$

Then the discrete Herglotz principle $\delta \mathcal{S}_d = 0$ for variations $\delta g_k \in T_{g_k} G$ vanishing at endpoints yields a discrete evolution whose image under the contact Legendre transform $\mathbb{FL} : TG \times \mathbb{R} \rightarrow T^*G \times \mathbb{R}$ coincides with the time- h contact Hamiltonian flow of the continuous system associated with L

In particular, if $\Phi_H^h : T^*G \times \mathbb{R} \rightarrow T^*G \times \mathbb{R}$ denotes the time- h flow of the contact Hamiltonian vector field X_H , and $\theta = dz - \langle p, g^{-1}dg \rangle$ is the canonical contact form on $T^*G \times \mathbb{R}$, then

$$(\Phi_H^h)^* \theta = \exp \left(\int_0^h (\partial_z H) \circ \Phi_H^t dt \right) \theta. \quad (32)$$

Equivalently, in first-order form at (g_k, p_k, z_k) ,

$$(\Phi_H^h)^* \theta = (1 + h \partial_z H(g_k, p_k, z_k) + O(h^2)) \theta. \quad (33)$$

Proof. We split the argument into two parts: first we show that the discrete Herglotz principle with L_h^e reproduces the sampled Euler–Poincaré–Herglotz flow, and then we derive the conformal factor for the contact form.

Step 1: Exact discrete Lagrangian and sampled flow. Fix $h > 0$ and consider a solution $(g(t), \xi(t), z(t))$, $t \in [0, h]$ of the Euler–Poincaré–Herglotz equations (28) with boundary data $g(0) = g_k$, $z(0) = z_k$, $g(h) = g_{k+1}$.

By definition,

$$L_h^e(g_k, g_{k+1}, z_k) = \int_0^h L(g(t), \xi(t), z(t)) dt.$$

Along the same solution we have $\dot{z}(t) = L(g(t), \xi(t), z(t))$, hence

$$z(h) - z(0) = \int_0^h L(g(t), \xi(t), z(t)) dt = L_h^e(g_k, g_{k+1}, z_k).$$

Identifying $z(0) = z_k$ and $z(h) = z_{k+1}$ gives exactly the recursion (31),

$$z_{k+1} = z_k + L_h^e(g_k, g_{k+1}, z_k).$$

Now consider a partition $t_k = kh$, $k = 0, \dots, N$, and a discrete path $\{g_k\}_{k=0}^N$ with fixed endpoints g_0, g_N and initial cost z_0 . For each k , let $(g_k^{\text{cont}}(t), \xi_k^{\text{cont}}(t), z_k^{\text{cont}}(t))$, $t \in [0, h]$, be the unique solution of (28) with $g_k^{\text{cont}}(0) = g_k$, $z_k^{\text{cont}}(0) = z_k$, and $g_k^{\text{cont}}(h) = g_{k+1}$, and define z_{k+1} by (31). Concatenating these segments yields a piecewise smooth curve $(g(t), \xi(t), z(t))$, $t \in [0, Nh]$, with $g(t_k) = g_k$ and $z(t_k) = z_k$. By uniqueness of solutions of (28), the resulting curve is in fact the restriction to $[0, Nh]$ of a global solution of the Euler–Poincaré–Herglotz equations with the given initial data.

Summing the relations $z_{k+1} - z_k = L_h^e(g_k, g_{k+1}, z_k)$ we obtain

$$z_N - z_0 = \sum_{k=0}^{N-1} L_h^e(g_k, g_{k+1}, z_k) = \mathcal{S}_d.$$

Thus the discrete action \mathcal{S}_d coincides with the total change in the cost accumulator:

$$\mathcal{S}_d = z_N - z_0.$$

In particular, the discrete Herglotz principle $\delta \mathcal{S}_d = 0$ is equivalent to the condition $\delta z_N = 0$ under variations $\delta g_k \in T_{g_k} G$ with $\delta g_0 = \delta g_N = 0$, since z_0 is fixed.

On the other hand, the continuous Herglotz variational principle for the contact Lagrangian L (in Euler–Poincaré–Herglotz form) states that $\delta z(T) = 0$ for all variations $\delta g(t)$ with $\delta g(0) = \delta g(T) = 0$ is equivalent to the system (28) on $[0, T]$. Applying this with $T = Nh$ and restricting to variations compatible with the discretization (i.e., encoded by variations of the nodes $\{g_k\}$) shows that

$$\delta z_N = 0 \iff (g(t), \xi(t), z(t)) \text{ solves (28) on } [0, Nh].$$

Therefore, critical discrete curves for \mathcal{S}_d are precisely the samples $\{(g(t_k), z(t_k))\}$ of solutions of the continuous Euler–Poincaré–Herglotz equations at times $t_k = kh$. Passing to momenta via the contact Legendre transform $\mathbb{F}L : G \times \mathfrak{g} \times \mathbb{R} \rightarrow G \times \mathfrak{g}^* \times \mathbb{R}$, and then to cotangent variables $(g, p, z) \in T^*G \times \mathbb{R}$ via left trivialization, we obtain that the induced discrete map on $T^*G \times \mathbb{R}$ is exactly the time– h contact Hamiltonian flow Φ_H^h of the Hamiltonian system associated with L .

Step 2: Conformal factor for the contact form. On the Hamiltonian side, the dynamics are governed by the contact Hamiltonian vector field X_H on $(T^*G \times \mathbb{R}, \theta)$, which satisfies

$$\mathcal{L}_{X_H} \theta = (\partial_z H) \theta.$$

Let Φ_H^t denote its flow. Differentiating the pullback of θ along the flow and using Cartan's formula gives

$$\frac{d}{dt} ((\Phi_H^t)^* \theta) = (\Phi_H^t)^* (\mathcal{L}_{X_H} \theta) = (\Phi_H^t)^* ((\partial_z H) \theta) = ((\partial_z H) \circ \Phi_H^t) (\Phi_H^t)^* \theta.$$

Thus, for each initial condition, $(\Phi_H^t)^* \theta$ solves a scalar linear ODE of the form

$$\frac{d}{dt} \alpha(t) = a(t) \alpha(t), \quad \alpha(0) = \theta,$$

with $a(t) = (\partial_z H) \circ \Phi_H^t$. The solution is

$$(\Phi_H^t)^* \theta = \exp \left(\int_0^t a(s) ds \right) \theta = \exp \left(\int_0^t (\partial_z H) \circ \Phi_H^s ds \right) \theta.$$

Evaluating at $t = h$ yields (32).

Finally, expanding the exponential for small h around $t = 0$ gives

$$\exp \left(\int_0^h (\partial_z H) \circ \Phi_H^t dt \right) = 1 + h \partial_z H(g_k, p_k, z_k) + O(h^2),$$

since $\Phi_H^0 = \text{id}$ and therefore $(\partial_z H) \circ \Phi_H^0 = \partial_z H(g_k, p_k, z_k)$. This proves (33). \square

Remark 9. The exact discrete contact Lagrangian L_h^e depends on the solution of a boundary-value problem for the Euler–Poincaré–Herglotz equations and is therefore not computable in closed form except in very special situations. Its main role is conceptual: it provides the “gold standard” against which practical approximations L_d can be designed and compared, ensuring that the resulting integrators are *contact-structure consistent*. This is analogous to the role of exact discrete Lagrangians in symplectic Lie–group variational integrators [24, 21, 23]. \diamond

Definition 1 (Order of a discrete contact integrator). Let $(g(t), p(t), z(t))$ denote the exact solution of the continuous contact Hamiltonian flow associated with L (equivalently, of the Euler–Poincaré–Herglotz equations in momentum variables), and let (g_k, p_k, z_k) be the output of a discrete contact variational integrator (with time step h) constructed from a discrete Lagrangian L_d . We say that the method has *order* r if, for fixed final time $T = Nh$,

$$\|(g_N, p_N, z_N) - (g(T), p(T), z(T))\| = \mathcal{O}(h^r) \quad (h \rightarrow 0),$$

where the norm is taken in any smooth local trivialisation of $T^*G \times \mathbb{R}$.

Theorem 3 (Order of the contact LGVI). *Let L_h^e be the exact discrete contact Lagrangian defined in (30), and let L_d be a discrete Lagrangian such that*

$$L_d(g_k, g_{k+1}, z_k) = L_h^e(g_k, g_{k+1}, z_k) + \mathcal{O}(h^{r+1}), \quad h \rightarrow 0, \quad (34)$$

uniformly in (g_k, g_{k+1}, z_k) on compact subsets.

Then the discrete flow generated by L_d via the discrete Herglotz principle (and its associated contact generating function S_d) yields an order- r approximation of the continuous Euler–Poincaré–Herglotz flow. In particular, the global error in (g_k, p_k, z_k) over a fixed interval $T = Nh$ is $\mathcal{O}(h^r)$.

Proof. We argue in two steps. First we show that the discrete flow induced by L_d has local truncation error $\mathcal{O}(h^{r+1})$ with respect to the exact flow of the Euler–Poincaré–Herglotz equations. Then we invoke standard stability results for one-step methods to obtain a global $\mathcal{O}(h^r)$ error bound.

Step 1: Local error via the exact discrete Lagrangian. Let X_H be the contact Hamiltonian vector field on $T^*G \times \mathbb{R}$ associated with the contact Lagrangian L and let Φ_H^t denote its flow. By Proposition 1, the exact discrete contact Lagrangian L_h^e generates, via the discrete Herglotz principle, a discrete map

$$F_h^e : T^*G \times \mathbb{R} \rightarrow T^*G \times \mathbb{R}$$

such that $F_h^e = \Phi_H^h$, i.e., F_h^e coincides with the exact time- h flow of the continuous Euler–Poincaré–Herglotz dynamics.

Let F_h^d denote the discrete map on $T^*G \times \mathbb{R}$ produced by the same discrete Herglotz principle but using L_d instead of L_h^e , with associated type-II contact generating function S_d . By assumption (34),

$$L_d(g_k, g_{k+1}, z_k) = L_h^e(g_k, g_{k+1}, z_k) + \mathcal{O}(h^{r+1}), \quad h \rightarrow 0,$$

uniformly on compact subsets. Since the definition of the type-II generating function simply adds the terms z_k and a bilinear pairing between p_{k+1} and a discrete state increment depending smoothly on (g_k, g_{k+1}) , the same estimate carries over to the discrete generating functions: if S_h^e denotes the (implicit) type-II generating function associated with L_h^e , then

$$S_d(g_k, p_{k+1}, z_k) = S_h^e(g_k, p_{k+1}, z_k) + \mathcal{O}(h^{r+1}), \quad h \rightarrow 0,$$

again uniformly on compact sets.

The discrete update maps F_h^e and F_h^d are defined implicitly by the stationarity conditions of their respective generating functions (discrete Herglotz principle / type-II formulation). In local coordinates on $T^*G \times \mathbb{R}$, these stationarity equations can be written in the form

$$\mathcal{F}^e(y_k, y_{k+1}, h) = 0, \quad \mathcal{F}^d(y_k, y_{k+1}, h) = 0,$$

where $y_k = (g_k, p_k, z_k)$ and $y_{k+1} = (g_{k+1}, p_{k+1}, z_{k+1})$. The functions \mathcal{F}^e and \mathcal{F}^d are smooth in their arguments and in h , and their difference satisfies

$$\mathcal{F}^d(y_k, y_{k+1}, h) = \mathcal{F}^e(y_k, y_{k+1}, h) + \mathcal{O}(h^{r+1}),$$

since the only difference comes from replacing L_h^e by L_d in the discrete variational principle (and hence in the corresponding first variations).

For fixed y_k lying on an exact trajectory, the implicit function theorem applies to \mathcal{F}^e (hyper-regularity of L ensures that the Jacobian with respect to y_{k+1} is invertible), yielding a smooth dependence $y_{k+1} = F_h^e(y_k)$. Perturbing \mathcal{F}^e by an $\mathcal{O}(h^{r+1})$ term perturbs the solution y_{k+1} by the same order. More precisely, one obtains

$$F_h^d(y_k) - F_h^e(y_k) = \mathcal{O}(h^{r+1}), \quad h \rightarrow 0,$$

uniformly for y_k in compact sets. Since $F_h^e = \Phi_H^h$, this shows that the local truncation error of the method defined by L_d satisfies

$$F_h^d(y_k) - \Phi_H^h(y_k) = \mathcal{O}(h^{r+1}),$$

for exact data $y_k = (g(t_k), p(t_k), z(t_k))$ at time $t_k = kh$.

Step 2: Global error estimate. The discrete contact variational integrator defined by L_d is a one-step method on the smooth finite-dimensional manifold $T^*G \times \mathbb{R}$. The vector field X_H is smooth, and for fixed final time T the exact solution $(g(t), p(t), z(t))$ remains in a compact subset of $T^*G \times \mathbb{R}$ for $t \in [0, T]$. In any smooth local trivialisation of $T^*G \times \mathbb{R}$ over such a compact set, the map F_h^d is uniformly Lipschitz in the state variable and smooth in h for h sufficiently small.

The standard convergence theorem for one-step methods for ODEs (see, e.g., [24, 21, 23] in the variational context, or any textbook result) states that a consistent one-step method with local truncation error $\mathcal{O}(h^{r+1})$ and uniform stability yields a global error $\mathcal{O}(h^r)$ over a fixed interval $[0, T]$. Applying this to F_h^d and the exact flow Φ_H^h gives

$$\|(g_N, p_N, z_N) - (g(T), p(T), z(T))\| = \mathcal{O}(h^r), \quad T = Nh, \quad h \rightarrow 0,$$

where the norm is taken in any smooth local trivialisation of $T^*G \times \mathbb{R}$. Therefore, the discrete flow generated by L_d via the discrete Herglotz principle has order r . \square

4.3 Retraction-based contact LGVI

In practice, the exact discrete contact Lagrangian is replaced by a computable approximation constructed from a *retraction map* $R : \mathfrak{g} \rightarrow G$ such that $R(0) = e$ and $dR_0 = \text{id}$, which locally approximates the exponential map.

Given consecutive states $(g_k, g_{k+1}) \in G \times G$ and a step size h small enough so that $g_k^{-1}g_{k+1}$ lies in the domain of R^{-1} , we define the discrete Lie-algebra increment

$$\xi_k := \frac{1}{h} R^{-1}(g_k^{-1}g_{k+1}) \in \mathfrak{g}. \quad (35)$$

A first-order retraction-based *contact discrete Lagrangian* is

$$L_d(g_k, g_{k+1}, z_k) := h L(g_k, \xi_k, z_k), \quad (36)$$

with higher-order midpoint or trapezoidal variants obtained by evaluating L at (g_{k+1}, ξ_k, z_k) or at a midpoint of the form

$$(g_k R(\tfrac{1}{2}h\xi_k), \xi_k, z_k + \tfrac{1}{2}h L(g_k, \xi_k, z_k)).$$

We lift the construction to the extended space $M := T^*G \times \mathbb{R}$, endowed with the discrete left-trivialized contact one-form

$$\Theta_k := dz_k - \langle p_k, g_k^{-1} dg_k \rangle, \quad (37)$$

which is the discrete analogue of the canonical contact form $\theta = dz - \langle p, g^{-1} dg \rangle$ in the Lie-group setting.

Given L_d , we define the associated *discrete contact generating function* of type II by

$$S_d(g_k, p_{k+1}, z_k) := z_k + L_d(g_k, g_{k+1}, z_k) + \langle p_{k+1}, R^{-1}(g_k^{-1} g_{k+1}) \rangle, \quad (38)$$

where g_{k+1} is viewed as a function of (g_k, p_{k+1}, z_k) through the critical point conditions and $R^{-1}(g_k^{-1} g_{k+1}) \in \mathfrak{g}$.

Theorem 4 (Contact LGVI on a Lie group). *Let L_d be defined by (36) and S_d by (38). Consider the discrete map $\Psi_k : (g_k, p_{k+1}, z_k) \mapsto (g_{k+1}, p_k, z_{k+1})$, where (g_{k+1}, p_k, z_{k+1}) is determined implicitly by*

$$\partial_{g_k} S_d = 0, \quad \partial_{p_{k+1}} S_d = 0, \quad z_{k+1} = z_k + L_d(g_k, g_{k+1}, z_k). \quad (39)$$

Then Ψ_k is a strict discrete contactomorphism:

$$\Psi_k^* \Theta_{k+1} = \Theta_k, \quad (40)$$

where Θ_k is given by (37). In particular, the LGVI preserves the discrete contact structure on $T^*G \times \mathbb{R}$ exactly.

Proof. Differentiating (38) and using the definition of Θ_k in (37) yields, on the extended space with coordinates $(g_k, p_k, z_k, g_{k+1}, p_{k+1}, z_{k+1})$, the discrete contact identity

$$dS_d = \Theta_k + \langle p_{k+1}, g_{k+1}^{-1} dg_{k+1} \rangle - \Theta_{k+1}, \quad (41)$$

which is the Lie-group analogue of the identity (16) in Section 3.

On the graph of the update map Ψ_k , the variables (g_{k+1}, p_k, z_{k+1}) are expressed in terms of (g_k, p_{k+1}, z_k) via (39) and the recursion for z_k . Restricting (41) to this graph, and using the relation $z_{k+1} = z_k + L_d(g_k, g_{k+1}, z_k)$ to eliminate dz_{k+1} , we obtain an identity of the form

$$dS_d = \Theta_k - \Psi_k^* \Theta_{k+1},$$

where S_d is now viewed as a function of the independent variables (g_k, p_{k+1}, z_k) .

Moreover, along a discrete trajectory generated by S_d the stationarity conditions (39) imply that the pullback of dS_d by Ψ_k vanishes, $\Psi_k^* dS_d = 0$.

Combining this with the previous identity yields

$$0 = \Psi_k^* dS_d = \Theta_k - \Psi_k^* \Theta_{k+1},$$

and hence $\Psi_k^* \Theta_{k+1} = \Theta_k$, which proves (40). \square

Remark 10. Theorem 4 is the contact analogue of Lie-group variational integrators as in [24, 21], now formulated on the extended contact manifold $T^*G \times \mathbb{R}$. It provides the geometric backbone for structure-preserving discrete PMP schemes on Lie groups, improving on purely coordinate-based discrete PMP formulations. \diamond

4.4 Discrete contact PMP on Lie groups

We now combine the contact LGVI with the discrete contact PMP of Section 3 for a control system on G . Let the controlled dynamics be given by

$$g_{k+1} = g_k R(h f(g_k, u_k)), \quad (42)$$

where $f : G \times U \rightarrow \mathfrak{g}$ is a left-trivialized control vector field and R is a retraction as above.

To avoid notational confusion with the discrete contact Lagrangian $L_d(g_k, g_{k+1}, z_k)$ of the LGVI, we denote the *discrete running cost* by

$$\ell_d : G \times U \rightarrow \mathbb{R}, \quad (g_k, u_k) \mapsto \ell_d(g_k, u_k),$$

and the terminal cost by $\Phi : G \rightarrow \mathbb{R}$.

We define the discrete contact Hamiltonian

$$H_d(g_k, p_{k+1}, z_k, u_k) := \left\langle p_{k+1}, \frac{1}{h} R^{-1}(g_k^{-1} g_{k+1}) \right\rangle + \ell_d(g_k, u_k) = \langle p_{k+1}, f(g_k, u_k) \rangle + \ell_d(g_k, u_k), \quad (43)$$

where g_{k+1} is given by (42), so that $R^{-1}(g_k^{-1} g_{k+1}) = h f(g_k, u_k)$ and both expressions coincide.

Theorem 5 (Discrete contact PMP on a Lie group). *Let $\{u_k^*\}_{k=0}^{N-1}$ be optimal for the discrete problem on G , with associated trajectory $\{(g_k^*, z_k^*)\}$. Assume normality of the extremal. Then there exists a nontrivial costate sequence $\{p_k^*\}_{k=1}^N \subset \mathfrak{g}^*$ such that, for each $k = 0, \dots, N-1$,*

1. *State and cost updates:*

$$g_{k+1}^* = g_k^* R(h f(g_k^*, u_k^*)), \quad (44a)$$

$$z_{k+1}^* = z_k^* + \ell_d(g_k^*, u_k^*). \quad (44b)$$

2. *Adjoint recursion (left-trivialized):*

$$p_k^* = \text{Ad}_{R(h f(g_k^*, u_k^*))}^* p_{k+1}^* + h \partial_g \ell_d(g_k^*, u_k^*), \quad (45)$$

where $\partial_g \ell_d(g_k^*, u_k^*) \in \mathfrak{g}^*$ denotes the left-trivial derivative of ℓ_d with respect to g .

3. *Terminal condition:*

$$p_N^* = d_g \Phi(g_N^*). \quad (46)$$

4. *Stationarity:*

$$u_k^* \in \arg \max_{u \in U} H_d(g_k^*, p_{k+1}^*, z_k^*, u), \quad (47)$$

with H_d given by (43).

Moreover, the optimal update map $\Psi_k : (g_k^*, p_{k+1}^*, z_k^*) \mapsto (g_{k+1}^*, p_k^*, z_{k+1}^*)$ is a discrete contactomorphism of $(T^*G \times \mathbb{R}, \Theta_k)$ with respect to the discrete contact one-form (37), in the sense of (40).

Proof. The proof follows the same finite-dimensional Lagrange multiplier argument as in Theorem 1, now in local trivializations of G . The discrete dynamics (42) play the role of the constraint map, and the multipliers λ_{k+1} live in the dual Lie algebra \mathfrak{g}^* after identification via charts and left trivialization. The adjoint recursion (45) is the intrinsic, left-trivialized version of the multiplier update, and the stationarity condition (47) is equivalent to $\partial_u H_d = 0$, hence to the maximum condition under the standing compactness and continuity assumptions (cf. Theorem 1). Finally, the contactomorphism property is inherited from Theorem 4, since the optimal update map is precisely the contact LGVI flow associated with the discrete generating function S_d augmented with the control-dependent term $\ell_d(g_k, u_k)$ in the cost accumulation. \square

Remark 11. The PMP on matrix Lie groups in [27] provides a geometric discrete PMP without explicit reference to contact geometry. Theorem 5 extends this viewpoint by showing that, when the discrete dynamics are generated by a contact LGVI, the discrete PMP update is automatically a contactomorphism on $T^*G \times \mathbb{R}$. In particular, the adjoint recursion (45) is consistent with the left-trivialized PMP in [27], but enjoys the additional property of preserving the discrete contact structure induced by the cost accumulation. \diamond

Corollary 1 (Abnormal discrete extremals on G). *If the Lagrange multiplier associated with the cost functional vanishes (abnormal case), the discrete contact PMP on G reduces to*

$$p_k^* = \text{Ad}_{R(hf(g_k^*, u_k^*))}^* p_{k+1}^*, \quad (\partial_u f(g_k^*, u_k^*))^* p_{k+1}^* = 0,$$

with no contribution from ℓ_d and Φ . Such extremals depend only on the geometry of the constraint $g_{k+1} = g_k R(hf(g_k, u_k))$ and are typically ruled out in practice by rank conditions on $\partial_u f$ which force triviality of the multiplier sequence. \diamond

5 Controlled Lindblad dynamics for a qubit

We now specialize the discrete contact PMP of Section 3 to a controlled open quantum system: a single qubit subject to Hamiltonian control and amplitude-damping Lindblad dissipation. The state space is the compact convex manifold

$$Q = \{\rho \in \mathbb{C}^{2 \times 2} : \rho^\dagger = \rho, \rho \geq 0, \text{tr}(\rho) = 1\},$$

equivalently the closed Bloch ball in \mathbb{R}^3 .

Let $\rho(t) \in Q$ denote the qubit density operator, written in the computational basis $\{|0\rangle, |1\rangle\}$. The dynamics of a Markovian open system with coherent control $u(t) \in \mathbb{R}$ and amplitude-damping noise are given by the Gorini–Kossakowski–Sudarshan–Lindblad (GKSL) master equation

$$\dot{\rho}(t) = \mathcal{L}_{u(t)}(\rho(t)) := -i[H(u(t)), \rho(t)] + \mathcal{D}(\rho(t)), \quad (48)$$

where \mathcal{L}_u is the Lindblad generator associated with the fixed control value u , acting linearly on density operators.

The coherent part is generated by the Hamiltonian

$$H(u) = \frac{u}{2} \sigma_x, \quad \sigma_x = \begin{pmatrix} 0 & 1 \\ 1 & 0 \end{pmatrix}.$$

For the purposes of this section we neglect any drift Hamiltonian; adding a fixed drift H_0 does not affect the structure of the PMP.

The dissipative part corresponds to the standard amplitude-damping channel with Lindblad operator

$$L = \sqrt{\gamma} \sigma_-, \quad \gamma > 0,$$

where

$$\sigma_- := |0\rangle \langle 1| = \begin{pmatrix} 0 & 0 \\ 1 & 0 \end{pmatrix}$$

is the lowering (decay) operator from the excited state $|1\rangle$ to the ground state $|0\rangle$. The corresponding GKSL dissipator is

$$\mathcal{D}(\rho) = L\rho L^\dagger - \frac{1}{2}\{L^\dagger L, \rho\}.$$

Thus the dynamics (48) preserve positivity and trace, as required for physical density operators.

We consider the following Bolza-type optimal control problem: for a fixed horizon $T > 0$, minimize the cost functional

$$J(u) = \int_0^T \alpha u^2(t) dt + \Phi(\rho(T)), \quad \alpha > 0, \quad (49)$$

subject to (48).

The terminal cost is chosen as

$$\Phi(\rho) = 1 - \text{tr}(\rho \rho_{\text{target}}), \quad \rho_{\text{target}} = |0\rangle \langle 0|.$$

Since $\text{tr}(\rho \rho_{\text{target}}) = \langle 0 | \rho | 0 \rangle$ is the fidelity with the ground state, one has $\Phi(\rho) = 0$ iff $\rho = \rho_{\text{target}}$ and $\Phi(\rho) > 0$ otherwise. The running cost $\alpha u^2(t)$ penalizes large control amplitudes and ensures the normality of the optimal extremal.

It is convenient to rewrite the dynamics in Bloch vector form. Let σ_y and σ_z denote the remaining Pauli matrices,

$$\sigma_y = \begin{pmatrix} 0 & -i \\ i & 0 \end{pmatrix}, \quad \sigma_z = \begin{pmatrix} 1 & 0 \\ 0 & -1 \end{pmatrix},$$

and write the density operator as

$$\rho = \frac{1}{2}(I + r \cdot \sigma) = \frac{1}{2}(I + r_x \sigma_x + r_y \sigma_y + r_z \sigma_z),$$

where I is the 2×2 identity, $r = (r_x, r_y, r_z)^\top \in \mathbb{R}^3$ is the Bloch vector, and $\sigma = (\sigma_x, \sigma_y, \sigma_z)$. Positivity and trace imply $\|r\| \leq 1$, so the state space is the closed Bloch ball $\mathbb{B}^3 = \{r \in \mathbb{R}^3 : \|r\| \leq 1\}$.

Substituting this parametrization into (48) and using standard Pauli algebra, one obtains the affine control system

$$\dot{r}(t) = A r(t) + b + u(t) B r(t), \quad (50)$$

with matrices

$$A = \begin{pmatrix} -\frac{\gamma}{2} & 0 & 0 \\ 0 & -\frac{\gamma}{2} & 0 \\ 0 & 0 & -\gamma \end{pmatrix}, \quad b = \begin{pmatrix} 0 \\ 0 \\ \gamma \end{pmatrix}, \quad B = \begin{pmatrix} 0 & 0 & 0 \\ 0 & 0 & -1 \\ 0 & 1 & 0 \end{pmatrix}.$$

Equivalently,

$$\begin{aligned} \dot{r}_x &= -\frac{\gamma}{2} r_x, \\ \dot{r}_y &= -\frac{\gamma}{2} r_y - u r_z, \\ \dot{r}_z &= -\gamma(r_z - 1) + u r_y = -\gamma r_z + \gamma + u r_y. \end{aligned} \quad (51)$$

The term $Ar + b$ describes amplitude-damping relaxation toward the ground state $r_{\text{target}} = (0, 0, 1)^\top$, while uBr is the Hamiltonian rotation generated by $H(u) = (u/2)\sigma_x$.

In Bloch coordinates, the cost functional (49) becomes

$$J(u) = \int_0^T \alpha u^2(t) dt + \Phi_{\text{Bloch}}(r(T)),$$

where a direct computation shows that

$$\Phi_{\text{Bloch}}(r) = 1 - \text{tr}\left(\frac{1}{2}(I + r \cdot \sigma) |0\rangle \langle 0|\right) = 1 - \frac{1}{2}(1 + r_z) = \frac{1}{2}(1 - r_z).$$

Thus, up to an affine rescaling, the terminal cost simply penalizes deviation of the z -component from its target value $r_z = 1$.

From the viewpoint of Section 3, we may regard either ρ or its Bloch representation r as the state variable x in the PMP, with dynamics $\dot{x} = f(x, u)$ given by (48) or (50), respectively, and running cost $L(x, u) = \alpha u^2$. In subsequent sections we discretize these dynamics using the contact Lie-group variational integrators of Section 4, and apply the discrete contact PMP to obtain structure-preserving optimal control schemes for the controlled Lindblad qubit.

Throughout, we use a *second-order accurate* contact LGVI and compare it against a classical second-order Runge–Kutta–Munthe–Kaas (RKMK(2)) method. Thus any numerical differences arise purely from geometry—in particular, preservation (or lack thereof) of discrete contact structure.

Let $U(t) \in \mathrm{SU}(2)$ evolve by

$$\dot{U}(t) = -iH(u(t))U(t), \quad U(0) = I. \quad (52)$$

For a constant control over a step $[t_k, t_{k+1}]$ of size Δt ,

$$U_{k+1} = \exp(-iH(u_k)\Delta t)U_k. \quad (53)$$

This is an exact Lie-group update of the type used in Runge–Kutta–Munthe–Kaas (RKMK) and commutator-free integrators [25, 19, 12]. Given U_{k+1} , the unitary subflow on density operators is

$$\rho_{k+1}^{(u)} = U_{k+1}\rho_kU_{k+1}^\dagger. \quad (54)$$

Following the standard operator-sum (Kraus) representation of completely positive trace-preserving (CPTP) quantum channels [20], any Markovian dissipative subflow admits an exact expression of the form

$$\Phi(\rho) = \sum_j E_j \rho E_j^\dagger, \quad \sum_j E_j^\dagger E_j = I.$$

For amplitude-damping noise, the Kraus operators are

$$E_0(\tau) = \begin{pmatrix} 1 & 0 \\ 0 & \sqrt{1-p(\tau)} \end{pmatrix}, \quad E_1(\tau) = \begin{pmatrix} 0 & \sqrt{p(\tau)} \\ 0 & 0 \end{pmatrix}, \quad p(\tau) = 1 - e^{-\gamma\tau}, \quad (55)$$

which yield the exact dissipative subflow

$$\Phi_{\mathrm{AD}}^\tau(\rho) = E_0(\tau)\rho E_0(\tau)^\dagger + E_1(\tau)\rho E_1(\tau)^\dagger.$$

To combine Hamiltonian and dissipative evolution, we use a symmetric Strang splitting [29]. If Φ_{AD}^t and $\Phi_u^t(\rho) = U(t)\rho U(t)^\dagger$ denote the exact subflows, the Strang composition

$$\Phi_{\Delta t}^{(2)} = \Phi_{\mathrm{AD}}^{\Delta t/2} \circ \Phi_u^{\Delta t} \circ \Phi_{\mathrm{AD}}^{\Delta t/2}$$

yields a time-reversible second-order accurate approximation of the full Lindblad evolution.

Using the exact Hamiltonian subflow $U_{k+1} = \exp(-iH(u_k)\Delta t)U_k$ and the analytic amplitude-damping subflow, the discrete contact update reads:

$$\rho_{k+\frac{1}{2}} = \Phi_{\mathrm{AD}}^{\Delta t/2}(\rho_k), \quad (56a)$$

$$\rho_{k+\frac{1}{2}}^{(u)} = U_{k+1}\rho_{k+\frac{1}{2}}U_{k+1}^\dagger, \quad (56b)$$

$$\rho_{k+1} = \Phi_{\mathrm{AD}}^{\Delta t/2}\left(\rho_{k+\frac{1}{2}}^{(u)}\right). \quad (56c)$$

This defines the discrete map

$$\rho_{k+1} = F^{(2)}(\rho_k, u_k),$$

which is C^∞ in (ρ, u) , symmetric, and second-order accurate:

$$\rho_{k+1} = \rho(t_k + \Delta t) + \mathcal{O}(\Delta t^2).$$

We equip the space of Hermitian matrices with the real Hilbert–Schmidt pairing $\langle A, B \rangle = \text{Re } \text{tr}(A^\dagger B)$, which is the natural duality pairing compatible with the contact construction of Sections 3–4. In Bloch coordinates this coincides with the Euclidean pairing on \mathbb{R}^3 .

The discrete extended dynamics are

$$\rho_{k+1} = F^{(2)}(\rho_k, u_k), \quad z_{k+1} = z_k + L_d(\rho_k, u_k),$$

where, consistently with the second-order accurate LGVI and with the theory of exact and approximate discrete contact Lagrangians, the discrete running cost is chosen as

$$L_d(\rho_k, u_k) = \alpha u_k^2 \Delta t + \mathcal{O}(\Delta t^3).$$

This corresponds to a second-order quadrature approximation of the continuous Lagrangian $L(\rho, u) = \alpha u^2$ and ensures overall second-order consistency of the discrete contact variational integrator.

Following the type-II discrete contact Hamiltonian formalism of Section 3, the discrete contact Hamiltonian is

$$H_d(\rho_k, P_{k+1}, z_k, u_k) := \langle P_{k+1}, F^{(2)}(\rho_k, u_k) \rangle + L_d(\rho_k, u_k), \quad (57)$$

while the difference

$$F^{(2)}(\rho_k, u_k) - \rho_k = \dot{\rho}(t_k) \Delta t + \mathcal{O}(\Delta t^2)$$

acts as a discrete approximation of the continuous state displacement, fully analogous to the term $F(x_k, u_k) - x_k$ in the discrete PMP. With this sign convention, the discrete contact PMP is formulated as a *maximization* of H_d with respect to the control, consistently with Theorem 1.

Remark 12 (Hamiltonian sign convention for minimization problems). The discrete contact Hamiltonian (57) has the generic PMP structure

$$H_d(\rho_k, P_{k+1}, z_k, u_k) = \langle P_{k+1}, F^{(2)}(\rho_k, u_k) \rangle + L_d(\rho_k, u_k),$$

so that minimization of the Bolza cost is achieved by *maximizing* H_d with respect to u_k .

For numerical purposes it is often convenient to work with an equivalent Hamiltonian of the form

$$\tilde{H}_d(\rho_k, P_{k+1}, u_k) := \langle P_{k+1}, F^{(2)}(\rho_k, u_k) - \rho_k \rangle - L_d(\rho_k, u_k),$$

which matches the usual “ $p \cdot (F - x) - L$ ” convention for minimization problems. Since the additional term $\langle P_{k+1}, \rho_k \rangle$ does not depend on u_k , both H_d and \tilde{H}_d yield the same maximizers and therefore the same PMP stationarity condition. In the numerical implementation of Section 6 we use \tilde{H}_d in the Hamiltonian maximization step, while the theoretical discrete PMP is written in terms of H_d in (57). \diamond

A corresponding type-II discrete contact generating function is

$$S_d(\rho_k, P_{k+1}, z_k, u_k) := z_k + L_d(\rho_k, u_k) + \langle P_{k+1}, F^{(2)}(\rho_k, u_k) - \rho_k \rangle,$$

where L_d is the discrete running cost introduced above.

Criticality of S_d with respect to (ρ_k, P_{k+1}) reproduces the discrete contact PMP conditions. Indeed, the equation $\partial_{P_{k+1}} S_d = F^{(2)}(\rho_k, u_k) - \rho_k$ recovers the discrete state update, while $\partial_{\rho_k} S_d$ yields the adjoint recursion. Similarly, the condition $\partial_{u_k} S_d = 0$ produces the discrete stationarity requirement for the optimal control. Thus S_d acts as a genuine type-II discrete contact generating function, and generates the discrete contactomorphism defining the optimal update

$$(\rho_k, P_{k+1}, z_k) \longmapsto (\rho_{k+1}, P_k, z_{k+1}),$$

in complete analogy with the Lie-group contact variational integrators developed in Section 4.

Proposition 2 (Discrete contact PMP for the Lindblad qubit). *Let $\{u_k^*\}_{k=0}^{N-1}$ be optimal for the discrete Bolza problem associated with the data $(F^{(2)}, L_d, \Phi)$, where*

$$\rho_{k+1} = F^{(2)}(\rho_k, u_k), \quad L_d(\rho_k, u_k) = \alpha u_k^2 \Delta t + \mathcal{O}(\Delta t^3),$$

and $\Phi(\rho) = 1 - \text{tr}(\rho \rho_{\text{target}})$. Then there exists a nontrivial sequence of Hermitian costates $\{P_k^*\}_{k=1}^N$ such that, for $k = 0, \dots, N-1$,

state and cost updates:

$$\rho_{k+1}^* = F^{(2)}(\rho_k^*, u_k^*), \quad z_{k+1}^* = z_k^* + L_d(\rho_k^*, u_k^*), \quad (58)$$

adjoint recursion:

$$P_k^* = \partial_\rho H_d(\rho_k^*, P_{k+1}^*, z_k^*, u_k^*), \quad k = 0, \dots, N-1, \quad (59)$$

terminal condition:

$$P_N^* = -\rho_{\text{target}}, \quad (60)$$

stationarity:

$$u_k^* \in \arg \max_{u \in U} H_d(\rho_k^*, P_{k+1}^*, z_k^*, u), \quad k = 0, \dots, N-1, \quad (61)$$

where the discrete contact Hamiltonian H_d is given by (57).

In particular, with the convention (57) the discrete PMP for the Lindblad qubit is naturally written as a maximization of H_d (or, equivalently, of \tilde{H}_d in Remark 12) for a minimization problem in Bolza form.

Proof. We apply the discrete contact PMP of Section 3 with state manifold Q equal to the convex set of qubit density operators, endowed with the real Hilbert–Schmidt pairing $\langle A, B \rangle = \text{Re} \, \text{tr}(A^\dagger B)$. By identifying covectors with Hermitian matrices via this pairing, a discrete covector $p_k \in T_{\rho_k}^* Q$ corresponds to a Hermitian matrix P_k such that $p_k(\delta\rho) = \langle P_k, \delta\rho \rangle$ for all Hermitian perturbations $\delta\rho$.

The discrete dynamics have the form

$$\rho_{k+1} = F^{(2)}(\rho_k, u_k), \quad z_{k+1} = z_k + L_d(\rho_k, u_k),$$

with $F^{(2)}$ the second-order Strang–split Lindblad integrator defined in (56) and L_d a second-order approximation of the running cost $\int_{t_k}^{t_{k+1}} \alpha u^2(t) dt$.

The general discrete contact PMP (Theorem 1) applied to the triple $(F^{(2)}, L_d, \Phi)$ yields the following conditions. First, the state and cost updates are those already stated above. Second, the adjoint variables satisfy the recursion

$$p_k = \partial_\rho L_d(\rho_k, u_k) + (\partial_\rho F^{(2)}(\rho_k, u_k))^* p_{k+1},$$

where $(\cdot)^*$ denotes the adjoint with respect to the Hilbert–Schmidt pairing. Third, the costate at the final time is fixed by the terminal condition $p_N = d_\rho \Phi(\rho_N)$. Finally, the optimal controls satisfy the discrete stationarity condition $u_k \in \arg \max_{u \in U} H_d(\rho_k, p_{k+1}, z_k, u)$, where the discrete contact Hamiltonian takes the form

$$H_d(\rho_k, p_{k+1}, z_k, u_k) = \langle p_{k+1}, F^{(2)}(\rho_k, u_k) \rangle + L_d(\rho_k, u_k),$$

which coincides with (57) when written in the matrix notation $p_{k+1} \leftrightarrow P_{k+1}$.

Since L_d does not depend on ρ_k , we have $\partial_\rho L_d(\rho_k, u_k) = 0$, and the adjoint recursion simplifies to

$$P_k = (\partial_\rho F^{(2)}(\rho_k, u_k))^* P_{k+1}. \quad (62)$$

This is precisely the form stated in the proposition, because

$$\partial_\rho H_d(\rho_k, P_{k+1}, z_k, u_k) = (\partial_\rho F^{(2)}(\rho_k, u_k))^* P_{k+1},$$

by differentiating (57) with respect to ρ_k .

For the terminal condition, we use $\Phi(\rho) = 1 - \text{tr}(\rho \rho_{\text{target}})$. A variation $\delta\rho$ gives

$$\delta\Phi(\rho) = -\text{tr}(\delta\rho \rho_{\text{target}}) = -\langle \rho_{\text{target}}, \delta\rho \rangle,$$

so, with respect to the Hilbert–Schmidt pairing, $d_\rho\Phi(\rho) = -\rho_{\text{target}}$, and hence $P_N^* = -\rho_{\text{target}}$.

Finally, the stationarity condition is exactly the specialization of the general maximization condition $u_k^* \in \arg \max_{u \in U} H_d(\rho_k^*, P_{k+1}^*, z_k^*, u)$ to the Hamiltonian (57). \square

Since L_d is independent of ρ , the adjoint recursion can be written directly as

$$P_k^* = (\partial_\rho F^{(2)}(\rho_k^*, u_k^*))^* P_{k+1}^*.$$

For the Strang–split update (56), the map $F^{(2)}$ is the composition

$$F^{(2)}(\cdot, u_k) = \Phi_{\text{AD}}^{\Delta t/2} \circ \mathcal{U}_{u_k} \circ \Phi_{\text{AD}}^{\Delta t/2}(\cdot),$$

where $\mathcal{U}_{u_k}(\rho) = U_k \rho U_k^\dagger$ with $U_k := \exp(-iH(u_k)\Delta t)$, and Φ_{AD}^τ is the amplitude–damping channel from (55). The derivative of a linear CPTP map is the map itself, and its adjoint with respect to the Hilbert–Schmidt pairing is the dual channel $\Phi_{\text{AD}}^{\tau*}$. For the unitary conjugation \mathcal{U}_{u_k} , the adjoint is $X \mapsto U_k^\dagger X U_k$. Therefore, the adjoint recursion (62) becomes

$$P_k^* = \Phi_{\text{AD}}^{\Delta t/2*} \left(U_k^\dagger \Phi_{\text{AD}}^{\Delta t/2*}(P_{k+1}^*) U_k \right), \quad U_k = \exp(-iH(u_k^*)\Delta t), \quad (63)$$

which is the explicit backward propagation of the costate through the Strang–split CPTP dynamics.

Remark 13. The map $(\rho_k, P_{k+1}, z_k) \rightarrow (\rho_{k+1}, P_k, z_{k+1})$ defined implicitly by the type–II generating function

$$S_d(\rho_k, P_{k+1}, z_k, u_k) := z_k + L_d(\rho_k, u_k) + \langle P_{k+1}, F^{(2)}(\rho_k, u_k) - \rho_k \rangle$$

is a strict discrete contactomorphism of the contact manifold $(T^*Q \times \mathbb{R}, \Theta)$, with $\Theta = dz - \langle P, d\rho \rangle$, by Theorem 2. Thus the Lindblad LGVI splitting scheme preserves both the quantum state space (complete positivity and trace preservation) and the discrete contact geometry induced by the cost accumulation. \diamond

To obtain a fair comparison with the contact LGVI of the previous section, we now introduce a standard *second–order* Runge–Kutta–Munthe–Kaas method (RKM(2)) applied to the Lindblad vector field $\dot{\rho} = \mathcal{L}_{u_k}(\rho)$ on the state manifold Q . Both schemes are Lie–group–based and second order, but—as we emphasize throughout this subsection—their geometric properties differ fundamentally.

In full analogy with the LGVI formulation $\rho_{k+1} = F^{(2)}(\rho_k, u_k)$, we write the RKM(2) update as

$$\rho_{k+1}^{\text{RKM}} = F_{\text{RKM}}(\rho_k, u_k),$$

where the map F_{RKM} is defined as follows. For a constant control u_k , let

$$\xi(\rho) := \mathcal{L}_{u_k}(\rho)$$

denote the Lindblad generator viewed as a linear operator on Q . The two–stage RKM(2) integrator is:

1. *Stage values:*

$$K_1 = \xi(\rho_k), \quad K_2 = \xi\left(\exp\left(\frac{1}{2}\Delta t K_1\right) \rho_k \exp\left(-\frac{1}{2}\Delta t K_1\right)\right).$$

2. *Update:*

$$\rho_{k+1}^{\text{RKMK}} = \exp(\Delta t K_2) \rho_k \exp(-\Delta t K_2). \quad (64)$$

Like the LGVI, this method uses a Lie–group exponential for the coherent subdynamics and is formally second order. Unlike the LGVI, however, the dissipative dynamics are incorporated only through the embedded algebra element K_2 , and therefore complete positivity and trace preservation are *not* guaranteed.

To place RKM(2) in direct parallel with the contact LGVI, we endow it with the *ordinary* discrete PMP structure. The discrete running cost is chosen with the same second–order accuracy as in the LGVI:

$$L_d^{(2)}(\rho_k, u_k) = \alpha u_k^2 \Delta t + \mathcal{O}(\Delta t^3),$$

which matches the approximation order of the continuous Lagrangian $L(\rho, u) = \alpha u^2$.

Mirroring the definition of the contact Hamiltonian H_d used in the LGVI, but *without* the contact term z , we set

$$H_d^{\text{RKMK}}(\rho_k, P_{k+1}, u_k) := \langle P_{k+1}, F_{\text{RKMK}}(\rho_k, u_k) \rangle + L_d^{(2)}(\rho_k, u_k). \quad (65)$$

This plays the same algebraic role as (57), but it is *not* a contact Hamiltonian.

In exact analogy with the LGVI update $(\rho_k, z_k) \mapsto (\rho_{k+1}, z_{k+1})$, the RKM extended dynamics read:

$$\rho_{k+1} = F_{\text{RKMK}}(\rho_k, u_k), \quad z_{k+1} = z_k + L_d^{(2)}(\rho_k, u_k).$$

Since $L_d^{(2)}$ is independent of ρ_k , the ordinary PMP yields

$$P_k = \partial_\rho H_d^{\text{RKMK}}(\rho_k, P_{k+1}, u_k) = (\partial_\rho F_{\text{RKMK}}(\rho_k, u_k))^* P_{k+1}.$$

This expression is structurally identical to the LGVI adjoint recursion, except that here the derivative acts on F_{RKMK} rather than on the Strang–split CPTP map $F^{(2)}$.

Here the parallelism with the LGVI stops:

$$(\rho_k, P_{k+1}, z_k) \longmapsto (\rho_{k+1}, P_k, z_{k+1})$$

is *not* generated by a type–II contact generating function. Consequently, the update is *not* a discrete contactomorphism; the discrete contact form $\Theta = dz - \langle P, d\rho \rangle$ is *not* preserved; and complete positivity and trace preservation are not enforced by the integrator.

In contrast, the contact LGVI enforces all three properties exactly.

Remark 14. Both integrators are second–order and both exploit Lie–group structure in the unitary dynamics. However, the LGVI is built from a discrete contact Lagrangian and a type–II discrete contact generating function, uses exact Kraus maps for dissipation, and yields a strict discrete contactomorphism preserving complete positivity, trace, and contact geometry.

The RKM(2) method, while formally similar in order and Lie–group handling, is not derived from any discrete Lagrangian or generating function. It therefore lacks exact dissipative structure, exact positivity, and discrete contact preservation.

Thus the two methods share order of accuracy but differ fundamentally in geometric fidelity—a distinction that becomes evident in the numerical experiments of Section 6. \diamond

6 Numerical results

In this section we illustrate the behaviour of the contact LGVI discretization developed in Section 5 and compare it with a second–order Runge–Kutta–type scheme (labelled RK2) applied directly to the Lindblad master equation. Both methods have order 2; the comparison is therefore focused on their *geometric* properties (CPTP structure, contact geometry), rather than on order of accuracy.

Throughout we consider the controlled amplitude–damping qubit of Section 5, with Hilbert space $\mathcal{H} = \mathbb{C}^2$, Hamiltonian $H(u) = \frac{u}{2}\sigma_x$ and dissipator $\mathcal{D}(\rho) = L\rho L^\dagger - \frac{1}{2}\{L^\dagger L, \rho\}$, $L = \sqrt{\gamma}\sigma_-$. Unless otherwise stated, the initial state is $\rho_0 = |1\rangle\langle 1|$, and the target state is $\rho_{\text{target}} = |0\rangle\langle 0|$.

6.1 Experimental set–up and performance metrics

The continuous dynamics are governed by the Lindblad equation

$$\dot{\rho}(t) = \mathcal{L}_{u(t)}(\rho(t)) := -i[H(u(t)), \rho(t)] + \mathcal{D}(\rho(t)). \quad (66)$$

For the numerical experiments we fix a terminal time T and a uniform grid $t_k = k\Delta t$, $k = 0, \dots, N$, with $N = T/\Delta t$. The control is chosen as a smooth pulse

$$u(t) = 4 \sin\left(\frac{\pi t}{T}\right), \quad (67)$$

and discretized as $u_k = u(t_k)$.

The “contact” scheme uses the second–order Strang splitting constructed in Section 5. On each time step the state update is

$$\rho_{k+\frac{1}{2}} = \Phi_{\text{AD}}^{\Delta t/2}(\rho_k), \quad (68a)$$

$$\rho_{k+\frac{1}{2}}^{(u)} = U_{k+1} \rho_{k+\frac{1}{2}} U_{k+1}^\dagger, \quad U_{k+1} = \exp(-iH(u_k) \Delta t), \quad (68b)$$

$$\rho_{k+1} = \Phi_{\text{AD}}^{\Delta t/2}(\rho_{k+\frac{1}{2}}^{(u)}), \quad (68c)$$

where Φ_{AD}^τ is the exact amplitude–damping channel with Kraus operators (55). Each step of this map is completely positive and trace preserving (CPTP) and defines the discrete dynamics $\rho_{k+1} = F_C^{(2)}(\rho_k, u_k)$ used inside the contact LGVI framework. The extended variables (P_k, z_k) are updated by the discrete contact PMP of Section 5, so that the extended map $(\rho_k, P_{k+1}, z_k) \mapsto (\rho_{k+1}, P_k, z_{k+1})$ is a strict discrete contactomorphism.

As non–contact reference we use an explicit second–order Runge–Kutta method of Heun type applied directly to the Lindblad generator,

$$\dot{\rho} = \mathcal{L}_{u(t)}(\rho) = -i[H(u(t)), \rho] + \mathcal{D}(\rho). \quad (69)$$

On each step we compute

$$\begin{aligned} k_1 &= \mathcal{L}_{u_k}(\rho_k), \\ k_2 &= \mathcal{L}_{u_{k+\frac{1}{2}}}(\rho_k + \frac{\Delta t}{2}k_1), \end{aligned}$$

and update

$$\rho_{k+1} = \rho_k + \frac{\Delta t}{2}(k_1 + k_2). \quad (70)$$

In the numerical experiments we set $u_{k+\frac{1}{2}} = u_k$, a standard simplification that preserves the global second–order accuracy of the Heun method.

This RK2 integrator is used purely as a non–geometric benchmark: it does *not* exploit the Kraus/CPTP structure of the Lindblad flow and is not guaranteed to preserve positivity, unit

trace, or the discrete contact form. Accordingly, the extended variables (P_k, z_k) are updated using the ordinary discrete PMP (i.e. without a contact generating function), so the RK2 extended map is not a discrete contactomorphism.

To obtain an accuracy benchmark we compute a ‘‘reference’’ trajectory $\rho_{\text{ref}}(t_k)$ using the contact LGVI integrator with a much smaller time step $\Delta t_{\text{ref}} = \Delta t/20$. For the time grids considered here this fine solution is visually indistinguishable from the exact Lindblad evolution.

For a given trajectory $\{\rho_k\}$ we monitor:

- *Trace drift:*

$$\delta_{\text{tr}}(k) := |\text{tr}(\rho_k) - 1|. \quad (71)$$

For a CPTP integrator this quantity should remain at roundoff level.

- *Positivity drift:* Let $\lambda_{\min}(\rho_k)$ denote the smallest eigenvalue of ρ_k . We define

$$\delta_{\text{pos}}(k) := -\min\{0, \lambda_{\min}(\rho_k)\}, \quad (72)$$

which vanishes exactly when ρ_k is positive semidefinite.

- *Global error vs. reference:*

$$\varepsilon_{\text{glob}}(k) := \|\rho_k - \rho_{\text{ref}}(t_k)\|_F. \quad (73)$$

- *Contact-form defect:*

$$\theta_k := (z_{k+1} - z_k) - \langle P_{k+1}, \rho_{k+1} - \rho_k \rangle, \quad (74)$$

where $\langle \cdot, \cdot \rangle$ denotes the Hilbert–Schmidt pairing. For an exact discrete contactomorphism we expect $\theta_k \equiv 0$ (up to floating-point roundoff). Thus, for the contact LGVI we expect θ_k to remain at machine precision, while for the non–contact scheme θ_k is unconstrained and typically grows with Δt and k .

6.2 Short–horizon accuracy and structure preservation

We first consider a moderately short horizon with weak damping $T = 10$, $\Delta t = 0.01$, $\gamma = 1$. Both integrators are initialized at $\rho_0 = |1\rangle\langle 1|$ and driven by the same control pulse $u(t) = 4 \sin(\pi t/T)$.

The ‘‘contact’’ scheme is the second–order Strang–split LGVI constructed in Section 5, which combines the exact unitary subflow generated by $H(u) = \frac{u}{2}\sigma_x$ with the exact amplitude–damping channel Φ_{AD}^τ in Kraus form. On each time step the state update is

$$\rho_{k+\frac{1}{2}} = \Phi_{\text{AD}}^{\Delta t/2}(\rho_k), \quad (75a)$$

$$\rho_{k+\frac{1}{2}}^{(u)} = U_{k+1} \rho_{k+\frac{1}{2}} U_{k+1}^\dagger, \quad U_{k+1} = \exp(-iH(u_k) \Delta t), \quad (75b)$$

$$\rho_{k+1} = \Phi_{\text{AD}}^{\Delta t/2}(\rho_{k+\frac{1}{2}}^{(u)}), \quad (75c)$$

where Φ_{AD}^τ is the exact amplitude–damping channel with Kraus operators (55). Each step of this map is completely positive and trace preserving (CPTP) and defines the discrete dynamics $\rho_{k+1} = F_C^{(2)}(\rho_k, u_k)$ used inside the contact LGVI framework. The extended variables (P_k, z_k) are updated by the discrete contact PMP of Section 5, so that the extended map $(\rho_k, P_{k+1}, z_k) \mapsto (\rho_{k+1}, P_k, z_{k+1})$ is a strict discrete contactomorphism.

As non–contact reference we use the explicit RK2 (Heun) method described in Section 6.1. This method evolves the same Lindblad generator \mathcal{L}_u , but it does not preserve positivity or unit trace exactly, nor does it preserve the discrete contact structure.

Figure 1 shows the Bloch trajectories of both schemes, obtained from $\rho_k = \frac{1}{2}(I + x_k\sigma_x + y_k\sigma_y + z_k\sigma_z)$. The contact LGVI and RK2 trajectories are qualitatively similar and remain close

Bloch trajectories ($T = 10, \Delta t = 0.01$)

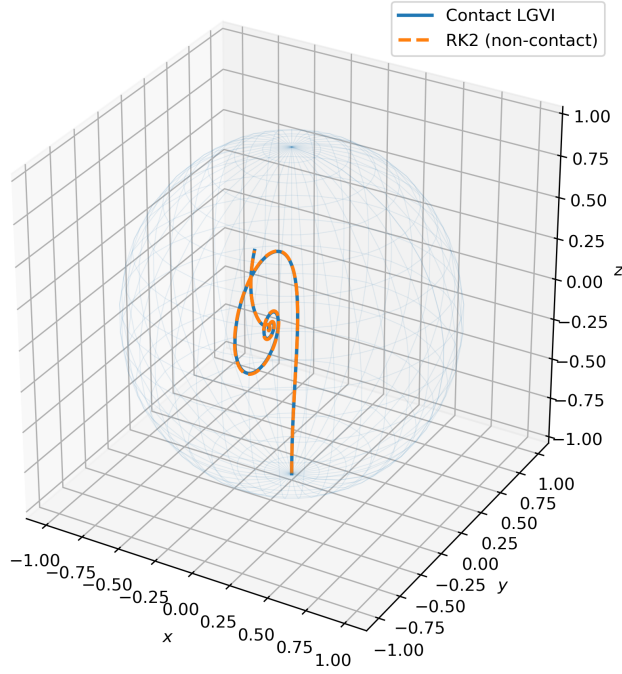


Figure 1: Bloch trajectories for $T = 10, \Delta t = 0.01$. Both schemes start from $\rho_0 = |1\rangle\langle 1|$ and are driven by the same sinusoidal control. The trajectories remain close and confined to the Bloch ball; the dynamics show the expected contraction towards the ground state.

to each other over the horizon; in both cases the dynamics display the expected contraction towards the ground state along the z -axis due to amplitude damping.

Figures 2 display the trace drift and positivity drift on a logarithmic scale. As expected, the contact LGVI preserves the trace at roundoff level and remains exactly positive semidefinite, with deviations compatible with machine precision. The RK2 method exhibits small but visible trace and positivity violations, which remain modest on this time scale but are already systematic.

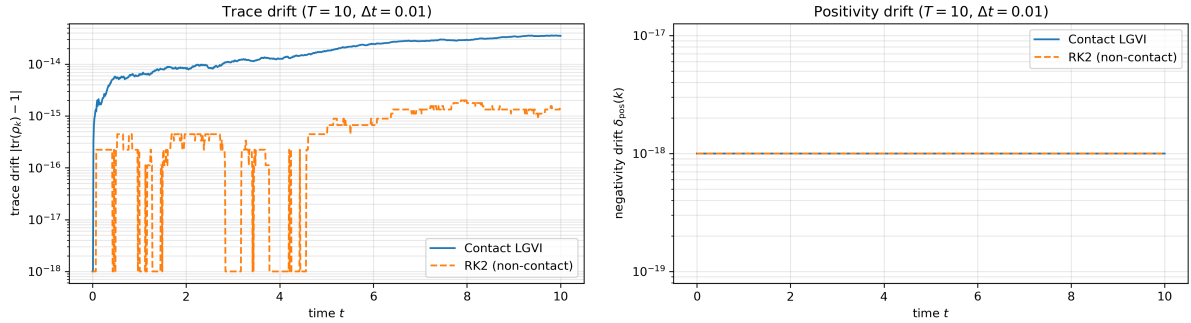


Figure 2: Left: Trace drift $|\text{tr}(\rho_k) - 1|$ for $T = 10, \Delta t = 0.01$. The contact LGVI keeps the trace at roundoff level, while RK2 exhibits a small but systematic drift, reflecting its lack of exact CPTP structure. Right: Positivity violation $\delta_{\text{pos}}(k)$ for $T = 10, \Delta t = 0.01$. The contact LGVI remains positive semidefinite to machine precision, whereas RK2 displays slight negativity in the eigenvalues of ρ_k .

Finally, Figure 3 shows the global error $\varepsilon_{\text{glob}}(k)$ with respect to the fine-step contact LGVI reference. Both methods display the expected second-order behaviour, with error growing smoothly over time. The contact LGVI achieves slightly smaller error constants, while at the

same time preserving CPTP structure exactly.

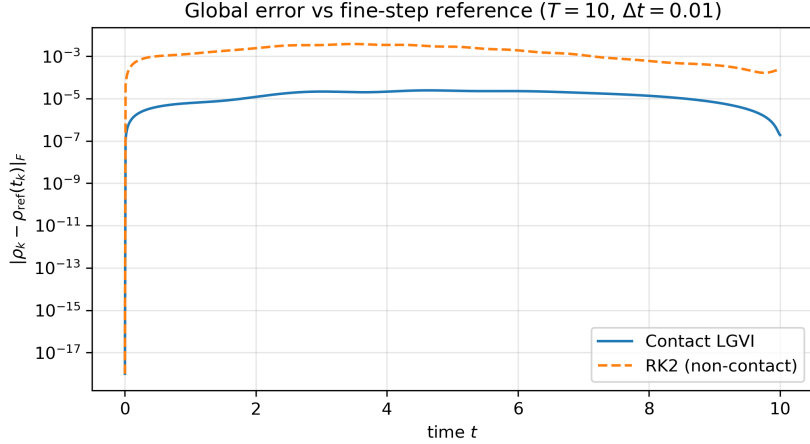


Figure 3: Global error $\varepsilon_{\text{glob}}(k) = \|\rho_k - \rho_{\text{ref}}(t_k)\|_F$ for $T = 10$, $\Delta t = 0.01$, using a fine-step contact LGVI trajectory as reference. Both schemes exhibit second-order accuracy; the contact LGVI has slightly smaller error while maintaining exact CPTP structure.

Overall, on short horizons both schemes are accurate and qualitatively consistent, but only the contact LGVI is exactly CPTP and contact-geometric at the discrete level.

6.3 Long-horizon stability

We now investigate numerical robustness on a longer horizon and under strong damping, a regime where geometric drift is most pronounced. We take $T = 100$, $\Delta t = 0.01$, $\gamma = 10$, leading to $N = 10^4$ steps. The initial state and control pulse are the same as in the previous experiment. For both schemes we compute the trace drift, positivity drift and contact-form defect.

The following table summarizes the observed maxima:

	$\max_k \delta_{\text{tr}}(k)$	$\max_k \delta_{\text{pos}}(k)$	$\max_k \theta_k $
Contact LGVI	8.9×10^{-14}	0	1.8×10^{-2}
RK2 (non-contact)	3.6×10^{44}	8.9×10^{60}	1.7×10^{64}

Figure 4 (left) shows the trace drift $\delta_{\text{tr}}(k) = |\text{tr}(\rho_k) - 1|$. The contact LGVI maintains the trace at roundoff level throughout the 10^4 -step evolution. In contrast, the non-contact RK2 scheme exhibits exponential blow-up, ultimately losing 40 orders of magnitude in trace preservation. Figure 4 (right) also displays the positivity drift $\delta_{\text{pos}}(k)$. The contact LGVI maintains positivity exactly up to floating-point noise, as expected from its CPTP structure. The RK2 method, lacking Kraus or CPTP constraints, rapidly produces negative eigenvalues whose magnitude eventually exceeds 10^{60} .

Finally, Figure 5 illustrates the magnitude of the contact-form defect

$$\theta_k := (z_{k+1} - z_k) - \langle P_{k+1}, \rho_{k+1} - \rho_k \rangle.$$

The contact LGVI scheme exhibits the expected $\mathcal{O}(\Delta t^2)$ level of defect (bounded by $\approx 10^{-2}$). The RK2 scheme, lacking a generating function or discrete contact structure, accumulates a defect that becomes astronomically large ($\sim 10^{64}$).

These results show that the contact LGVI discretization preserves CPTP structure and contact geometry even under strong dissipation and long horizons. The non-contact RK2 method, although second-order accurate in principle, becomes numerically nonphysical: it loses trace, breaks positivity, and drifts away from the contact-form identity by dozens of orders of magnitude.

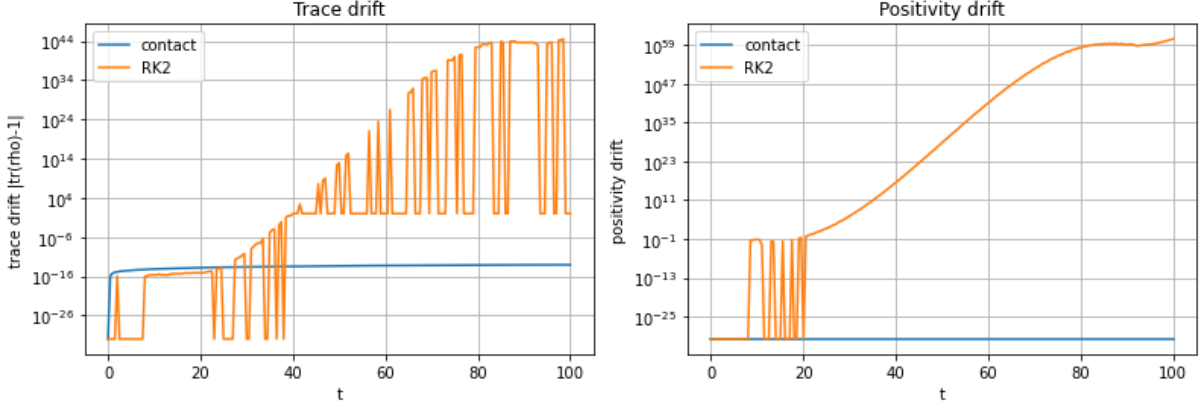


Figure 4: Left: Trace drift for $T = 100$, $\Delta t = 0.01$, $\gamma = 10$. The contact LGVI remains at machine precision, whereas the RK2 method loses trace preservation catastrophically. Right: Positivity drift for $T = 100$, $\Delta t = 0.01$, $\gamma = 10$. The contact LGVI stays positive semidefinite; RK2 produces massive violations of positivity

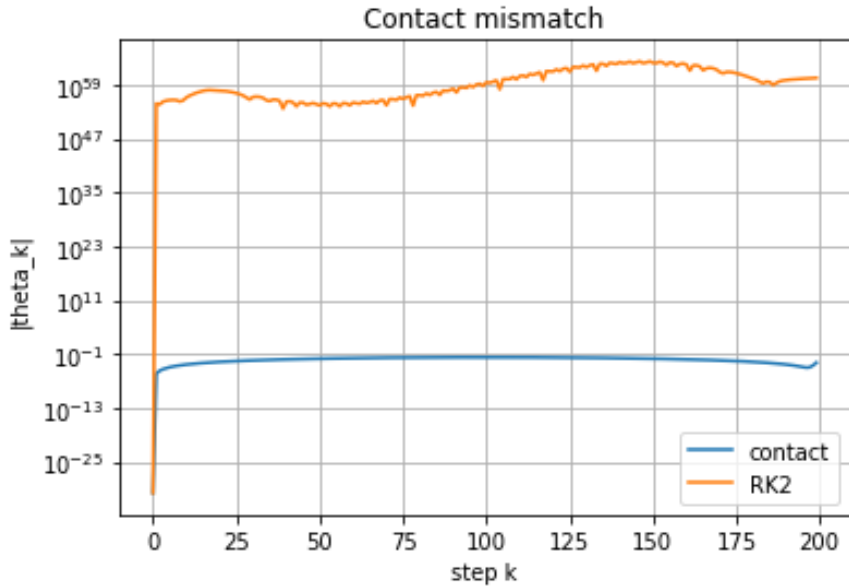


Figure 5: Contact-form defect θ_k for $T = 100$, $\Delta t = 0.01$, $\gamma = 10$. LGVI remains geometrically consistent; RK2 diverges dramatically.

This experiment confirms that geometric preservation is essential for robust long-horizon simulations of open quantum systems.

We evaluate robustness for a long horizon with strong dissipation ($T = 100$, $\Delta t = 0.01$, $\gamma = 10$). Across 10^4 time steps, the contact LGVI remains numerically CPTP: the trace stays at roundoff ($\sim 10^{-13}$), positivity is preserved exactly, and the contact-form defect remains bounded at the expected $\mathcal{O}(\Delta t^2)$ level ($\sim 10^{-2}$). This behaviour is consistent with the theoretical geometric guarantees of the scheme. In contrast, the non-contact RK2 discretization becomes rapidly nonphysical over the same horizon. Trace errors grow to $\mathcal{O}(10^{44})$, positivity is violated with negative eigenvalues of size $\mathcal{O}(10^{60})$, and the contact-form defect reaches $\mathcal{O}(10^{64})$. Thus, even though both integrators have formal order 2, only the contact LGVI maintains geometric consistency over long horizons when simulating open quantum systems with dissipation.

6.4 Optimal control with the discrete contact PMP

We now assess the impact of the integrator choice on the solution of an optimal control problem solved via a discrete Pontryagin Maximum Principle. We consider the same controlled amplitude-damping qubit as in Section 5, with parameters $T = 3$, $\Delta t = 0.01$, $\gamma = 1$, $\alpha = 0.05$, and box-constrained controls $u_k \in [-u_{\max}, u_{\max}]$ with $u_{\max} = 6$. The initial and target states are $\rho_0 = |1\rangle\langle 1|$ and $\rho_{\text{target}} = |0\rangle\langle 0|$. The Bolza cost is

$$J(u) = \sum_{k=0}^{N-1} \alpha u_k^2 \Delta t + \Phi(\rho_N), \quad \Phi(\rho) = 1 - \text{tr}(\rho \rho_{\text{target}}).$$

At each iteration of the PMP shooting algorithm we propagate the state, cost, and costate forward and backward in time, and update the control via maximization of the discrete Hamiltonian $H_d(\rho_k, P_{k+1}, u)$. We compare two discretizations:

- **Contact LGVI + discrete contact PMP:** the state update is the CPTP Strang map $F_C^{(2)}$, the cost and costate follow the discrete contact relations derived in Section 5, and the extended update $(\rho_k, P_{k+1}, z_k) \mapsto (\rho_{k+1}, P_k, z_{k+1})$ is a strict *discrete contactomorphism*.
- **RK2 (non-contact) + ordinary discrete PMP:** the state is propagated by an explicit second-order Runge–Kutta scheme of Heun type applied to the Lindblad generator, and the costate follows the corresponding RK2 adjoint recursion. This scheme is *not* CPTP and *not* a contactomorphism.

Both PMP solvers start from the *same* initial guess for the control,

$$u_k^{(0)} = 4 \sin\left(\frac{\pi t_k}{T}\right), \quad t_k = k\Delta t,$$

and use identical relaxation $\beta = 0.5$.

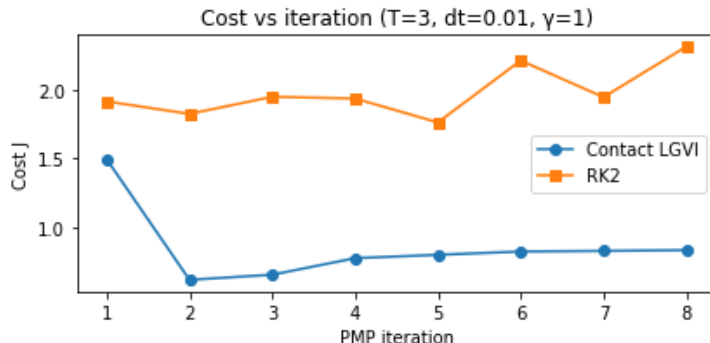


Figure 6: Evolution of the cost J over the PMP iterations for $T = 3$, $\Delta t = 0.01$, $\gamma = 1$, $\alpha = 0.05$. The contact LGVI (solid line) displays a regular decrease and converges to a slightly lower cost, whereas the RK2 discretisation (dashed line) shows a more oscillatory behaviour and settles at a higher value of J .

Figure 6 shows the evolution of the cost J over the first few shooting iterations for both discretisations. The **contact LGVI** produces a regular, almost monotone decrease of the cost and quickly reaches a plateau, indicating a stable convergence of the PMP iteration to a locally optimal control. The **RK2** discretisation, in contrast, exhibits a more oscillatory behaviour: the cost decreases more slowly and typically settles at a slightly higher value than the contact scheme.

In other words, on this short horizon both methods do converge to reasonable controls, but the LGVI-based PMP attains a marginally better objective and a more stable iteration, while the RK2-based PMP shows a less regular cost profile and tends to stagnate earlier.

The final optimal trajectories of each scheme are evaluated using the geometric metrics introduced in Section 6.1. Here the difference between the two discretisations is much more pronounced.

For the **contact LGVI**, we observe that

$$\max_k |\text{tr}(\rho_k) - 1| \approx 10^{-15}, \quad \max_k \delta_{\text{pos}}(k) = 0,$$

i.e., trace and positivity are preserved up to machine precision along the whole PMP trajectory. The contact-form defect

$$\theta_k = (z_{k+1} - z_k) - \langle P_{k+1}, \rho_{k+1} - \rho_k \rangle$$

remains at the expected $\mathcal{O}(\Delta t^2)$ scale, with typical values around

$$\max_k |\theta_k| \sim 10^{-3}.$$

For the **RK2** scheme, the optimal trajectories are no longer geometrically consistent. In a representative run we obtain

$$\max_k \delta_{\text{pos}}(k) \sim 10^{-3}, \quad \max_k |\theta_k| \sim 10^{-1},$$

so that RK2 violates positivity and the discrete contact identity by two to three orders of magnitude more than the contact LGVI, despite having the same nominal order of accuracy.

Figures 7 and 8 illustrate, respectively, the resulting optimal control pulses and the geometric drifts (contact-form defect and positivity drift) along the optimal trajectories.

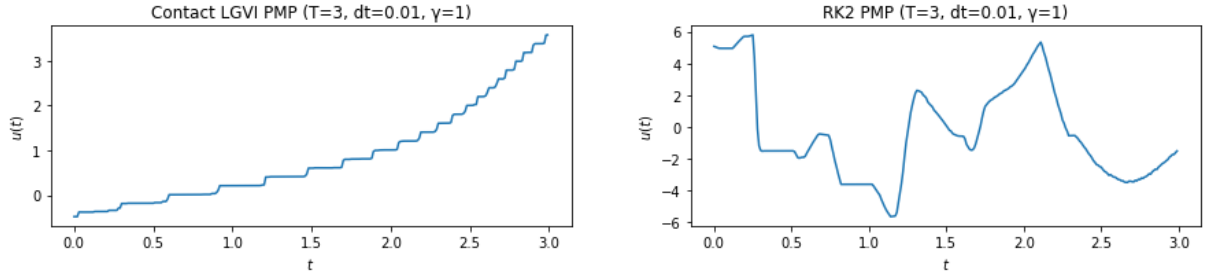


Figure 7: Optimal control pulses for $T = 3$, $\Delta t = 0.01$. Left: contact LGVI PMP; right: RK2 PMP. The contact scheme yields smooth pulses and consistent convergence; the RK2 scheme oscillates and fails to reach a comparable optimum.

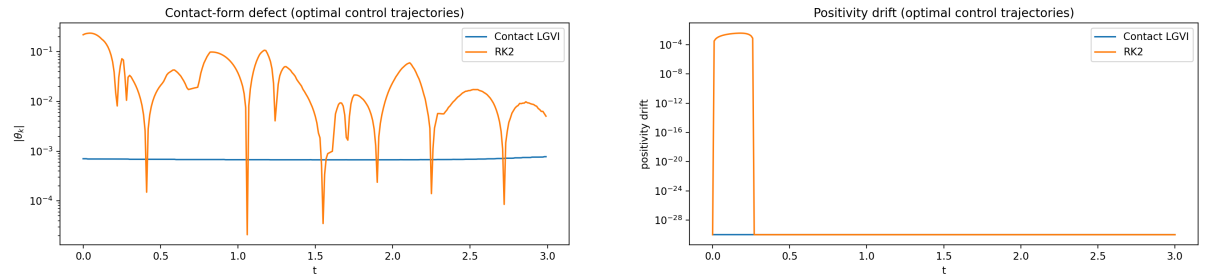


Figure 8: Geometric drifts along the optimal control trajectories. Left: contact-form defect $|\theta_k|$. Right: positivity drift $-\min\{0, \lambda_{\min}(\rho_k)\}$. The contact LGVI remains at machine precision and $\mathcal{O}(\Delta t^2)$; RK2 exhibits two to three orders of magnitude larger violations.

Overall, this experiment confirms that the discrete contact PMP equipped with the contact LGVI provides a robust and geometrically consistent method for optimal control of dissipative quantum systems. Even though both schemes are formally second order, the non-contact RK2 discretization fails to preserve CPTP structure and contact geometry, and this degradation directly harms the convergence and reliability of the PMP shooting iteration.

7 Conclusions and outlook

We have developed a discrete geometric framework for optimal control of open quantum systems governed by Lindblad dynamics, based on the contact formulation of the Pontryagin Maximum Principle and Lie–group variational integrators.

At the continuous level, the PMP for systems with running costs naturally lives on a contact manifold, with the state, costate, and cost variables evolving according to a contact Hamiltonian flow. We have shown that this structure admits a faithful discrete counterpart: starting from a discrete Herglotz principle, we constructed a discrete contact PMP on manifolds, and then lifted it to Lie groups by means of retractions and exact discrete contact Lagrangians. The resulting Lie–group contact variational integrators are generated by type–II discrete contact Hamiltonians and yield strict discrete contactomorphisms on the extended phase space.

We then specialized this construction to a single qubit subjected to Hamiltonian control and amplitude–damping noise. For this Lindblad system we designed a second–order contact LGVI that combines the exact Kraus map of the dissipative channel with the exact unitary evolution through a symmetric Strang splitting. By construction, each time step is completely positive and trace–preserving (CPTP) and preserves the discrete contact form associated with the cost accumulation. This provides a fully geometric discretization of the Lindblad PMP: the state, costate and cost variables evolve through an explicit discrete contactomorphism generated by a type–II discrete generating function.

For comparison, we considered a standard explicit second–order Runge–Kutta (Heun) integrator applied directly to the Lindblad generator. This RK2 scheme has the same formal order of accuracy as the contact LGVI but is not derived from a discrete Lagrangian or generating function, and does not enforce CPTP structure nor discrete contact geometry.

Our numerical experiments illustrate the consequences of these geometric differences. On short horizons with moderate damping, both schemes achieve comparable state–space accuracy, but only the contact LGVI maintains machine–precision trace and positivity, and exhibits a small contact–form defect consistent with the expected $\mathcal{O}(\Delta t^2)$ behaviour. On long horizons and under strong dissipation, the contrast becomes dramatic: the RK2 discretization develops catastrophic trace and positivity violations, together with a contact–form defect that grows by many orders of magnitude, while the contact LGVI remains numerically CPTP and contact–consistent throughout. When embedded in a discrete PMP shooting algorithm for a qubit optimal control problem, the contact LGVI leads to stable convergence towards physically meaningful optimal pulses, whereas the RK2–based PMP suffers from degraded performance and reduced reliability.

These results support the conclusion that contact–preserving geometric integrators are not merely aesthetically appealing, but practically advantageous for discrete optimal control of open quantum systems, especially when long horizons, dissipation, and variational principles interact.

Several directions for future work are opened by this study. On the theoretical side, it would be natural to construct higher–order contact LGVIs, to analyze their backward error and modified contact structure, and to extend the discrete contact PMP to more general classes of constraints and state–dependent running costs. On the physical side, applying the present framework to multi–qubit systems, collective dissipation, and more complex noise models (e.g. dephasing or finite–temperature baths) would further test its robustness and scalability. Finally, combining contact LGVIs with advanced numerical optimization methods (e.g. quasi–Newton or second–order techniques) and with experimental constraints from quantum hardware constitute an interesting avenue towards geometric, hardware–compatible optimal control for noisy intermediate–scale quantum devices.

References

- [1] C. Altafini and F. Ticozzi, “Modeling and control of quantum systems: An introduction,” *IEEE Transactions on Automatic Control*, vol. 57, no. 8, pp. 1898–1917, 2012.
- [2] A. Anahory Simoes, D. Martín de Diego, M. de León, and M. Lainz. On the geometry of discrete contact mechanics. *Journal of Nonlinear Science*, 31:88, 2021.
- [3] A. Anahory, L. J. Colombo, M. de León, J. C. Marrero, D. M. de Diego, and E. Padrón, Reduction by symmetries of contact mechanical systems on Lie groups. *SIAM Journal on Applied Algebra and Geometry*, 8(4), 821–845, 2024.
- [4] M. A. P. Assif, D. Chatterjee, and R. Banavar. A simple proof of the discrete-time geometric Pontryagin maximum principle on smooth manifolds. *Automatica*, 114:108847, 2020.
- [5] M. Barbero-Liñán and M. C. Muñoz-Lecanda. Geometric approach to Pontryagin’s maximum principle. *Acta Applicandae Mathematicae* 108.2 (2009): 429–485.
- [6] S. Blanes and F. Casas. Splitting methods for nonautonomous separable dynamical systems. *Journal of Physics A: Mathematical and General*, 39(19):5405–5423, 2006.
- [7] V. G. Boltyanskii, *Optimal Control of Discrete Systems*, John Wiley & Sons, New York, 1978.
- [8] B. Bonnard, M. Chyba, and D. Sugny, Time-minimal control of dissipative two-level quantum systems: The generic case. *IEEE Transactions on Automatic Control*, 54(11):2598–2610, 2009.
- [9] B. Bonnard, O. Cots, N. Shcherbakova, and D. Sugny, The energy minimization problem for two-level dissipative quantum systems. *Journal of Mathematical Physics*, 51(9):092705, 2010.
- [10] B. Bonnard and D. Sugny, Geometric optimal control and two-level dissipative quantum systems. *SIAM Journal on Control and Optimization*, 48(3):1289–1308, 2009.
- [11] H.-P. Breuer and F. Petruccione, *The Theory of Open Quantum Systems*. Oxford University Press, 2002.
- [12] E. Celledoni, H. Marthinsen, and B. Owren. An introduction to Lie group integrators—basics, new developments and applications. *Journal of Computational Physics*, 257(B), 1040–1061, 2014.
- [13] W. Clark, A. M. Bloch, L. J. Colombo, and P. Rooney, Optimal control of quantum purity for $n = 2$ systems. In *Proc. IEEE CDC*, pp. 1317–1322, 2017.
- [14] W. Clark, A. M. Bloch, L. J. Colombo, and P. Rooney, Optimal control of quantum purity for two-level dissipative systems. *DCDS-S*, pp. 2357–2372, 2019.
- [15] M. de León, M. Lainz, and M. C. Muñoz-Lecanda. Optimal control, contact dynamics and Herglotz variational problem. *Journal of Nonlinear Science*, 33(9):1–46, 2023.
- [16] H. Geiges, *An Introduction to Contact Topology*. Cambridge University Press, 2008.
- [17] V. Gorini, A. Kossakowski, and E. C. G. Sudarshan, Completely positive dynamical semi-groups of N -level systems. *Journal of Mathematical Physics*, 17(5):821–825, 1976.
- [18] E. Hairer, C. Lubich, and G. Wanner, *Geometric Numerical Integration: Structure-Preserving Algorithms for Ordinary Differential Equations*, 2nd ed., Springer Series in Computational Mathematics, Vol. 31, Springer, Berlin, 2006.

- [19] A. Iserles, H. Z. Munthe-Kaas, S. P. Nørsett, and A. Zanna. Lie-group methods. *Acta Numerica*, 9:215–365, 2000.
- [20] K. Kraus, *States, Effects and Operations: Fundamental Notions of Quantum Theory*. Lecture Notes in Physics, Vol. 190, Springer, 1983.
- [21] M. Leok and T. Shingel, General techniques for constructing variational integrators. *Frontiers of Mathematics in China*, 7 (2012), 273–303.
- [22] G. Lindblad. On the generators of quantum dynamical semigroups. *Communications in Mathematical Physics*, 48:119–130, 1976.
- [23] J. C. Marrero, D. Martín de Diego, and E. Martínez, Local convexity for second order differential equations on a Lie algebroid. arXiv:2103.14418, 2021.
- [24] J. E. Marsden and M. West, Discrete mechanics and variational integrators. *Acta Numerica*, 10:357–514, 2001.
- [25] H. Munthe-Kaas, Runge–Kutta methods on Lie groups. *BIT Numerical Mathematics*, 38(1):92–111, 1998.
- [26] T. Ohsawa. Contact geometry of the Pontryagin maximum principle. *Automatica*, 51:40–46, 2015.
- [27] K. S. Phogat, D. Chatterjee, and R. Banavar. A discrete-time Pontryagin maximum principle on matrix Lie groups. *Automatica*, 68:207–216, 2016.
- [28] R. T. Rockafellar, Lagrange multipliers and optimality. *SIAM Review*, 35(2):183–238, 1993.
- [29] G. Strang. On the construction and comparison of difference schemes. *SIAM Journal on Numerical Analysis*, 5(3):506–517, 1968.
- [30] M. Vermeeren, A. Bravetti, and M. Seri. Contact variational integrators. *Journal of Physics A*, 52(44):445206, 2019.
- [31] H. M. Wiseman and G. J. Milburn, *Quantum Measurement and Control*, Cambridge University Press, 2009.